TAMPERE UNIVERSITY OF TECHNOLOGY

MASOUMEH HASANI

OPTIMIZATION OF THE CLOSE COUPLING EFFECT FOR PASSIVE UHF RFID TAGS IN STACKED APPLICATIONS

Master of Science Thesis

Examiners: Professor Leena Ukkonen and
Professor Lauri Sydänheimo
Examiners and topic approved by the Faculty
Council of the Faculty of Computing and
Electrical Engineering on 5th December 2012.

Abstract

TAMPERE UNIVERSITY OF TECHNOLOGY
Master's Degree Programme in Electrical Engineering
HASANI, MASOUMEH: Optimization of the close coupling effect for passive UHF RFID tags in stacked applications
Master of Science Thesis, 73 pages,
May 2013
Major: Radio Frequency Electronics Engineering
Examiners: Professor Leena Ukkonen and Professor Lauri Sydänheimo
Keywords: Close coupling, UHF RFID, stacked application, Web tag, UofA

The use of the radio frequency identification has become more popular in recent years, since it has many advantages (such as operation without human involvement or detection non-line-of sight at several meters) than the other identification system. The RFID tags are utilized in many different applications. In a wide range of applications (e.g. in the retail business), the RFID tags are often stacked together. The stacked UHF RFID tags are known to have less read range compare to the stand-alone tags. In the other words, placing the tag in the close proximity of other tags, affects the performance of the tag, due to electromagnetic interference between the antennas of the tags. The most of the analysis about effect of the close coupling have been done for the UHF RFID tags in near-field application. Since many different factors are involved in the performance of the tag in far-field applications, it is more complicated to analyze the interaction between the tags when they are placed in the close proximity of each other inside the far-field region of the reader antenna.

In this project, the effect of some design parameters on the close coupling has been studied and one practical approach for improvement of the performance of the tags in the stacked application has been introduced. The performance of a reference tag in stack is measured. Then the new versions of the reference tag are designed by adjusting some of the reference tag antenna's parameters. The measurement of the new version designs in stack shows the performance enhancement for one of the new design. The comparison between the results of the different designs verifies that the design parameters can have influence to the minimizing of the close coupling effect.

Preface

This Master of Science Thesis is conducted in Smartrac Technology Finland Co., between September 2012 and February 2013. The objective of this master thesis is to study the close coupling effect of the passive UHF RFID tags in the far-field application. All the measurements and development are done in the Radio Frequency Laboratory of the Smartrac, Tampere.

The advancement of the thesis is supervised by Tuomas Koskelainen, RF project engineer, and the head of R&D CoE Tampere, Harri Aalto. The examiners of the Master of Science Thesis are Professor Leena Ukkonen and Professor Lauri Sydänheimo.

I would like to thank the examiners for their support, encouragement and valuable guidance during the whole thesis process.

I would also like to thank Tuomas Koskelainen, and Harri Aalto, for pushing forward during the thesis. Your valuable experiences, flexibility and encouragement made me motivated throughout the whole thesis work. In addition, I would like to thank all my colleagues in the Smartrac, Tampere, especially the R&D members for their continuous support and peaceful.

And my particular thanks to my family for their love and invaluable support. Last but not least, my warmest thanks to Dr. Ville Syrjälä for his love and caring.

Tampere, February 2013

Masoumeh Hasani

Contents

Abbreviations

AIDC	Automatic Identification and Data Capture
ASK	Amplitude-Shift Keying
CST	Computer Simulation Technology
CW	Carrier Wave
DSB	Double-Sideband
EPC	Electronic Product Code
ETSI	Europe Telecommunications Standards Institute
FCC	Federal Communications Commission
FDTD	Finite-Different Time-Domain
FEM	Finite Element Method
HF	High-Frequency
HPBW	Half-Power Beam Width
IC	Integrated Circuit
ISO	International Organization of Standards
LF	Low-Frequency
NFC	Near Field Communication
PIE	Pulse Interval Encoding
PR-ASK	Phase-Reverse Amplitude-Shift Keying
PSK	Phase Shift Modulation
RCS	Radar Cross Section
RFID	Radio Frequency Identification
SI	International System of Unit
UHF	Ultra-High Frequency
UID	Unique Identification Number
UofA	University of Arkansas
WORM	Write Once Read Many

Symbols

A_e	Effective aperture [m^2]
c	Speed of light [m/s]
D	Directivity [dBi]
e	Radiation efficiency
f	Frequency [1/s]
G	Gain [dBi]
P	Power [W]
R	Resistance [Ω]
U	Radiation intensity [W/sr]
X	Reactance [Ω]
Z	Impedance [Ω]
λ	Wavelength [m]
α	Attenuation constant [Np/m]
β	Phase constant [rad/m]
γ	Complex propagation constant [1/m]
Γ	Voltage reflection coefficient
ω	Angular frequency [rad/s]

Chapter 1

1. Introduction

The radio frequency identification (RFID) is one of many Automatic Identification and Data Capture (AIDC) methods that use propagation of electromagnetic waves for transferring information. In any RFID system, the identification is based on the electromagnetic interaction between the tags and the readers. All the objects that should be identified are labelled with the RFID tags and the reader communicates wirelessly with the tags to collect the appropriate information stored in them. The RFID tag consists of an integrated circuit (IC) that stores the data, and allows the backscattering communication and an antenna (attached to the substrate material) that is used for RF communication with the reader. A common reader includes a radio frequency module, a control unit and an antenna for communication with the tags. Comparing to the barcode system, another example of AIDC for labelling the items, the RFID system is getting more popular due to reliability, longer read range, carrying more information and operation without human involvement. RFID system has been utilized in various applications, such as handling global supply chain management, tracking systems, access control, inventory control, ID badges and near field communication (NFC) which is one of newest area for using RFID systems.

1.1. Motivation of Thesis

In wide range of the applications the RFID tags are utilized in stack or close proximity to other tags, during communication with the reader. For example, in a retail cloth stores, T-shirts or jeans which are labelled with tags, are in the stack on top of each other and reader should be able to identify them one by one. In such a case, it is probable that tags interfere with each other and reader is not easily able to identify all of them. Regarding to the distance between the tags in the stacked environment, the number of the tags, the design features of the tags and type of the reader, the intensity of the performance drop can be different. However, design of a tag that can perform in the

stack as well as a single inlay is one way to improve the system performance in these types of applications.

The characteristics and performance of the RFID tags are different with respect to the applications and the environments they are utilized. For instance, if an ordinary tag is stuck on metal, the read range rate decreases remarkably, since the electromagnetic interaction will arise at the antenna of the tag. Therefore, when few tags whose antennas are metal become close each other, the effect of coupling between the tag's antennas will change some of the characteristics of the tags (impedance mismatch and destructive interferences) and cause the weak performance of the tags. Here, the performance analysis of tags in close proximity to other tags is studied, only from tag antenna design point of view.

The objective of this thesis is to study the behaviour of the passive UHF RFID tag in close proximity of other tags and finding the parameters that have influence to the close coupling effect. In addition, by evaluating the effect of design parameters on this phenomenon, an example of optimal design to minimize the effect of the close coupling is introduced.

In this thesis, the modelling of the close coupling is based on the fact that, when the tags are close to each other, the tag antenna's impedance will change due to the electromagnetic coupling of antennas and presence of mutual impedance. This causes change of the received power by the tags and the reader which in most of the cases decreases the read range. This performance drop is verified by simulation and measurement results. In addition, some of the design parameters that have influence on the close coupling effect are discussed by introducing a new version design

1.2. Thesis Outlines

This thesis consists of 6 chapters. Chapter 2 discusses in detail the required theoretical background including, the electromagnetism equations, power, energy and propagation of electromagnetic wave, the basic of the antenna theory and a general review of the RFID system. In Chapter 3, design consideration of a passive UHF RFID tag antenna is provided and design process of an example tag is explained. In addition, close coupling effect, as a limiting factor in performance of tag antenna is introduced in chapter 3. In Chapter 4 attention is paid to the modelling of tags in the stacked environment and description of theoretical model of coupling between the tags. Moreover, the theoretical model is verified by simulation for few of the cases. The measurement of the simulated cases, improvement of the design and finding the optimal design for minimizing the close coupling effect, are discussed in Chapter 5. Finally, Chapter 6 summarizes the work presented in this thesis and draws the conclusion.

Chapter 2

2. Background Theory

2.1. Electromagnetic Theory

Study of electromagnetic theory will help to understand many of phenomena which take place in electrical engineering. In order to know how an antenna radiates or receives the signals, first should be understood how an electromagnetic wave propagates in different media. For this purpose, need to study about definition of electric and magnetic fields, and know what a field is. Considering all these concepts in detail is out of the scope of this thesis so part of relevant concepts to the thesis topic will be introduced here.

This section will start with a brief review of Maxwell's equations which are fundamental law and together with the theory of electromagnetism can explain on a macroscopic scale the properties of the electromagnetic fields. Then, the behaviour of the electromagnetic fields in different media will be studied and also the concept of energy and power density of the electromagnetic field is introduced. Finally, the propagation of the electromagnetic wave as a plane wave is considered in the last part

2.1.1. Maxwell's equations

Publication of James Clerk Maxwell in 1873 unified the electric and magnetic phenomena in a common view. Before that it was thought that there is no relation between electric and magnetic field and they are two separate concepts but Maxwell's equations, which use Gauss, Faraday's and Ampere's law as a base, were formulated to state the relationship between electric and magnetic fields. Basically it says if there is a time-varying electric field in a region there will be also a time-varying magnetic field in the same region [1]. In order to present the Maxwell's equation, some key quantities which are used to describe the time-varying vector field need to be introduced. The quantities are real functions of spatial coordinates (x, y, z) and the time coordinate (t) and according the International System of Unit (SI) they are defined in Table 1. Key rel-

Table 1. A partial list of field quantities [1] [2].

Quantity	Variable	Unit
Electric field intensity	$\overline{E}$	V/m
Magnetic field intensity	$\overline{H}$	A/m
Electric flux density	$\overline{D}$	C/m^2
Magnetic flux density	$\overline{B}$	Wb/m^2
Electric current density	$\overline{J}$	A/m^2
Magnetic current density	$\overline{M}$	V/m^2
Magnetic vector potential	$\overline{A}$	Wb/m
Electric charge density	ρ	C/m^3
Permeability	μ	H/m
Permittivity	ε	F/m
Conductivity	σ	S/m

ations between the field intensities and flux densities in the vacuum are defined as

$$\overline{D} = \varepsilon_0 \overline{E}\,, \tag{2.1}$$

$$\overline{B} = \mu_0 \overline{H}\,, \tag{2.2}$$

$$\overline{J} = 0 \tag{2.3}$$

where $\varepsilon_0 = 8.85\times10^{-12}$ F/m is dielectric constant of free air and $\mu_0 = 4\pi\times10^{-7}$ H/m refers permeability of free space [3].

Maxwell's equations are four second order partial differential equations that make a relation between electric field ($\overline{E}$), magnetic field ($\overline{B}$), charge (ρ) and current ($\overline{J}$). These four equations are usually represented in both differential and integral forms. Maxwell modified the Ampere's law for time-varying fields so the modified Ampere's law, two Gauss laws and Faraday's law of induction are called Maxwell's equation.

First equation, which based on Gauss' law for time-varying electric field, implies that the total electric flux density ($\overline{D}$) exiting a closed surface (of any volume) is equal to total charge density (ρ) inside the volume. Differential and integral forms of equation are given by

$$\nabla \cdot \overline{D} = \rho\,, \tag{2.4}$$

$$\int_{\partial V} \overline{D} \cdot d\overline{s} = \int_{V} \rho \cdot dv = Q \;\forall\, V \tag{2.5}$$

here, "$\nabla\cdot$" is the divergence and "$\cdot$" refers the dot product.

Second Maxwell's equation comes from Gauss's law for time-varying magnetic field. The equation says that magnetic flux density through a close surface is zero and there are no magnetic monopoles. In terms of mathematical equations, this can be written as

$$\nabla \cdot \overline{B} = 0\,, \tag{2.6}$$

$$\int_{\partial V} \overline{B} \cdot d\bar{s} = 0 \;\forall\, V\,. \tag{2.7}$$

The third equation, which is also a statement of Faraday's law, states that the electromotive force around a closed loop is produced by the rate of change of time varying magnetic flux through the circuit. Differential and integral forms of this equation are expressed mathematically as follows

$$\nabla \times \overline{E} = -\frac{\partial \overline{B}}{\partial t} \tag{2.8}$$

$$\int_{\partial S} \overline{E} \cdot d\bar{l} = -\frac{\delta}{\delta t} \int_{S} \overline{B} \cdot d\bar{s} \;\forall\, S \tag{2.9}$$

where "$\nabla \times$" is the curl operator.

The last Maxwell's equation with the contribution of Ampere's law is given as follow (both differential and integral forms)

$$\nabla \times \overline{H} = \overline{J} + \frac{\partial \overline{D}}{\partial t}\,, \tag{2.10}$$

$$\int_{\partial S} \overline{H} \cdot d\bar{l} = \int_{S} \overline{J} \cdot d\bar{s} + \frac{\delta}{\delta t} \int_{S} \overline{D} \cdot d\bar{s} \;\forall\, S \tag{2.11}$$

and it says that at any point in a medium, sum of displacement current density ($\partial \overline{D} / \partial t$) and conduction current density ($\overline{J}$) gives rise to a magnetic field that circles the currents.[1]

In most of the cases of analyzing time-varying electromagnetic fields, time-harmonic (sinusoidal) fields can be used. For a time-harmonic field we can use Phasor analysis and get single-frequency steady-state response and by using linear combination of single-frequency response we can get the complete response of time-varying sinusoidal field [1]. A time-harmonic real electric field can be presented as

$$\overline{E}(x, y, z, t) = \mathrm{Re}[\tilde{E}(x, y, z)\, e^{j\omega t}] \tag{2.12}$$

where $\tilde{E}(x, y, z)$ is Phasor form of time-harmonic electric field ($\overline{E}$) at any point of region. In the Eq. (2.12), $e^{j\omega t}$ shows the time dependency of the field and space dependency is included in $\tilde{E}$ [1]. By using the same approach for other field vectors

which were presented in Table 1, we can obtain the Phasor form of Maxwell's equations as follows

$$\nabla \cdot \tilde{D} = \rho, \tag{2.13}$$

$$\nabla \cdot \tilde{B} = 0, \tag{2.14}$$

$$\nabla \times \tilde{E} = -j\omega\tilde{B}, \tag{2.15}$$

$$\nabla \times \tilde{H} = \tilde{J} + j\omega\tilde{D}. \tag{2.16}$$

We must keep in mind that the electromagnetic fields must satisfy the Maxwell's equations as the condition for their existence [1].

If we suppose a region where there are a time-varying electric field ($\overline{E}$) and magnetic field ($\overline{B}$), when a charge q is moving with velocity of $\overline{u}$ in this region, the charge experiences force $\overline{F}$

$$\overline{F} = q(\overline{E} + \overline{u} \times \overline{B}) \tag{2.17}$$

this equation is known as Lorentz force equation and that is also one of significant equations to explain the effect of electromagnetism.[1]

2.1.2. Field in different media and boundary conditions

In previous section (Eq.(2.1) and (2.2)) we considered the relationships between field intensities and flux densities only in vacuum, while in the real application of electromagnetic system we have to analyze the behaviour of electromagnetic fields at the interface of different materials which have different properties. Boundary conditions are set of equations which explain the behaviour of fields on either side of an interface [1]. So it is necessary to explain the boundary conditions which should be applied on field vectors at the boundary of two materials to see how the field pattern on either side of a boundary would be.

First of all, the interface might be between two different dielectric materials or between a conductor and a dielectric, and the following conditions are always be valid,

- On the surface of a perfect conductor ($\sigma = \infty$), both ρ_s and $\overline{J}_s$ can exist since the electromagnetic fields inside a perfect conductor are zero.
- At the boundary between a conductor ($\sigma < \infty$) and a perfect dielectric, $\overline{J}_s$ is zero but ρ_s can exist since time-varying fields can exist inside a conductor.
- At the boundary between two perfect dielectrics ($\sigma = 0$), $\overline{J}_s$ is always zero. Also ρ_s is zero unless charge physically is placed at the interface. [2]

If we suppose that the unit vector $\overline{a_n}$, which is normal to the interface point from medium 2 to medium 1, then boundary conditions that the field vectors $\overline{E}$, $\overline{H}$, $\overline{D}$ and

$\overline{B}$ must satisfy at the interface of medium 1 and 2 are given as

- The normal components of the electric flux density ($\overline{D}$) are discontinuous at the interface of the two media where charge density ρ_s exists [1],

$$\overline{a_n} \cdot (\overline{D_1} - \overline{D_2}) = \rho_s, \tag{2.18}$$

  Eq. (2.18) can be derived from the first Maxwell's equation.
- The normal component of magnetic flux density ($\overline{B}$) is continuous across the interface [1]

$$\overline{a_n} \cdot (\overline{B_1} - \overline{B_2}) = 0 \tag{2.19}$$

  and from the 2nd Maxwell's equation we can prove the Eq (2.19).
- Similarly, the tangential component of the electric field ($\overline{E}$) is continuous at the interface [1]

$$\overline{a_n} \times (\overline{E_1} - \overline{E_2}) = 0, \tag{2.20}$$

  Eq.(2.20) can drive from the 3rd Maxwell's equation.
- The tangential component of the magnetic field ($\overline{H}$) is discontinuous at the interface of two medium where the surface current density $\overline{J_s}$ exists [1]

$$\overline{a_n} \times (\overline{H_1} - \overline{H_2}) = \overline{J}_s \tag{2.21}$$

  and the 4th Maxwell's equation proves the Eq.(2.21).

When we are looking for solution of Maxwell's equations in two media, we must verify that the fields are matched at the interface of two medium.

Finally, the equations which relate the electromagnetic fields to the properties of the material which the field exist are named constitutive equations. For an isotropic (μ and ε are independent of direction), linear (characteristics of the media does not depend on the strength of electric and magnetic fields) and non-dispersive (phase velocity of wave does not depend on its frequency) media the constitutive equations are given by [2]

$$\overline{D} = \varepsilon \overline{E}, \tag{2.22}$$

$$\overline{B} = \mu \overline{H}, \tag{2.23}$$

$$\overline{J} = \sigma \overline{E} \tag{2.24}$$

where ε, μ and σ are the permittivity, permeability and conductivity of the media respectively. The constitutive equations and Maxwell's equations, together with the Lorentz force equation form the foundation of electromagnetic theory and they can explain all macroscopic electromagnetic phenomena [1].

2.1.3. Energy and power

An electromagnetic system has energy which is stored into electric and magnetic fields. This energy will be transported through space over long distance and part of it (in terms of power) can be dissipated because of the loss. In this section, the relation between the rate of such energy transfer and the electromagnetic fields associated with it is discussed.

For a volume V is closed by surface S and contains electric and magnetic fields, in steady-state sinusoidal condition, the time-average electric energy that is stored in this volume is given by [2]

$$W_e = \frac{1}{4}\mathrm{Re}\int_V \overline{E}\cdot\overline{D}^{*}\, dv \tag{2.25}$$

and the time-average magnetic energy stored in the same volume is defined as [2]

$$W_m = \frac{1}{4}\mathrm{Re}\int_V \overline{H}\cdot\overline{B}^{*}\, dv \tag{2.26}$$

Eq.(2.25) and (2.26) for a lossless, isotropic, homogeneous and linear media where ε and μ can be considered as linear and scalar constant values, can be simplified to [2]

$$W_e = \frac{\varepsilon}{4}\int_V \overline{E}\cdot\overline{E}^{*}\, dv\,, \tag{2.27}$$

$$W_m = \frac{\mu}{4}\int_V \overline{H}\cdot\overline{H}^{*}\, dv\,. \tag{2.28}$$

If we suppose that the electric and magnetic source current ($\overline{J}_s$ and $\overline{M}_s$) are available inside the volume V, then in a lossy case (which means ε and μ can be complex) form Poynting power balance equation (which is explained in detail in [2]), three different power terms will be extracted. They are defined as follows

$$P_s = -\frac{1}{2}\int_V (\overline{E}\cdot\overline{J_s}^{*} + \overline{H}^{*}\cdot\overline{M}_s)\, dv \tag{2.29}$$

Eq. (2.29) is the complex power flow out of the surface S [2].

$$P_o = \frac{1}{2}\oint_s \overline{E}\times\overline{H}^{*}\cdot ds \tag{2.30}$$

This term refers the time-average power flow out the surface S for time-harmonic fields [2].

$$P_l = \frac{\sigma}{2}\int_V \left|\overline{E}\right|^2 dv + \frac{\omega}{2}\int_V (\varepsilon''\left|\overline{E}\right|^2 + \mu''\left|\overline{H}\right|^2)\, dv \tag{2.31}$$

Eq. (2.31) is the time-average lost power flow out the surface S [2]. Now concerning mentioned equations, the Poynting's theorem can be written as [2]

$$P_s = P_o + P_l + 2j\omega (W_m - W_e) \text{ [2].} \tag{2.32}$$

Poynting's theorem as a fundamental statement for energy conservation of the electromagnetic field implies that the power delivered by the source P_s is summation of the power transmitted through the surface P_o, the lost power in volume P_l and 2ω times of the net reactive energy stored in the volume [2].

2.1.4. Plane wave

From pervious section we know that, the Maxwell's equations include all necessary information for characterizing the electromagnetic fields at any point of medium. In order to study the behaviour of the waves, from Maxwell's equations we obtain an equation in term of one unknown variable, which is known as wave equation. Study the solution of the wave equations, gives useful information about wave propagation in medium. Generally, the electromagnetic fields is generated by time-varying source, propagate as a spherical wave. But if we consider these fields in a small region and so far away from radiating source, then spherical wave maybe approximated as a plane wave [1]. Actually, a plane wave propagates along a fixed direction of spatial coordinates (let's say z direction), so it has one-dimensional spatial dependency and does not have any field component in its direction of propagation. In the other words, the fields components of a plane wave lie in a transverse plane which is perpendicular to the direction of propagation of the wave [1].

Wave equations

A uniform medium is defined as a linear, isotropic and homogeneous (same medium properties in all directions) media with scalar constant of μ and ε [3]. In a uniform and source-free medium ($\overline{J}, \rho$ are zero) with the parameters μ, ε and σ, by applying the Maxwell's equations in term of two variable ($\overline{E}$, $\overline{H}$), the wave equation can be obtained as

$$\nabla^2 \overline{E} = \mu\sigma \frac{\partial \overline{E}}{\partial t} + \mu\varepsilon \frac{\partial^2 \overline{E}}{\partial t^2}, \tag{2.33}$$

$$\nabla^2 \overline{H} = \mu\sigma \frac{\partial \overline{H}}{\partial t} + \mu\varepsilon \frac{\partial^2 \overline{H}}{\partial t^2} \text{ [1].} \tag{2.34}$$

These equations can control the behaviour of all electromagnetic field in a uniform and source-free conducting medium.

Plane wave in a dielectric medium

In order to find the solutions of the wave equations, we will start with simple case of wave propagation in loss-less medium ($\sigma = 0$). In a dielectric medium, the wave equations simplified as

$$\nabla^2 \overline{E} = \mu\varepsilon \frac{\partial^2 \overline{E}}{\partial t^2}, \tag{2.35}$$

$$\nabla^2 \overline{H} = \mu\varepsilon \frac{\partial^2 \overline{H}}{\partial t^2} \text{ [1].} \tag{2.36}$$

The Eq. (2.35) and (2.36) are named time-dependent Helmholtz equations. If we suppose that the plane wave propagates in z direction, there are no field components in this direction so $E_z = 0$ and $H_z = 0$. Also, for a uniform (no variation for field in x and y direction) plane wave, $\partial / \partial x$ and $\partial / \partial y$ of field components are equal to zero [2]. Considering these conditions for time-harmonic fields, we can write the Phasor form of Eq.(2.35) as follows

$$\frac{d^2 \tilde{E}}{dz^2} + \omega^2 \mu\varepsilon \tilde{E}_x = 0 \tag{2.37}$$

where $\tilde{E}_x(z)$ is Phasor form of $E_x(z,t)$ and $\omega = 2\pi f$ [rad/s] is angular frequency of the wave [1]. If we define the quantity of β as phase constant

$$\beta = \omega\sqrt{\mu\varepsilon} \tag{2.38}$$

then, Eq. (2.37) is rewritten as

$$\frac{d^2 \tilde{E}}{dz^2} + \beta^2 \tilde{E}_x = 0 \text{ [1].} \tag{2.39}$$

Two independent solutions can be found for Eq. (2.39), and by substituting those in equation, the whole solution for time harmonic case is given as [2]

$$E_x(z) = E^+ e^{-j\beta z} + E^- e^{j\beta z} \tag{2.40}$$

where E^+ and E^- are arbitrary amplitude constant and will be determine by boundary conditions. Time domain form of Eq. (2.40) can be written as

$$E_x(z,t) = E^+ \cos(\omega t - \beta z) + E^- \cos(\omega t + \beta z). \tag{2.41}$$

Considering the first term of the Eq. (2.41), it refers the wave travelling in forward ($+z$) direction and the second term represents the wave travelling in backward ($-z$) direction. Since $\overline{E}$ and $\overline{H}$ are related together by Maxwell's equations, when we know the $\overline{E}$ field, we can obtain the $\overline{H}$ field

$$H_y = \frac{1}{\eta}(E^+ e^{-j\beta z} + E^- e^{j\beta z}) \tag{2.42}$$

where $\eta = \omega\mu / \beta$ is wave impedance and in free space is about 377 Ω [1]. The phase velocity of the wave is defined as

$$v_p = \frac{\omega}{\beta} = \frac{1}{\sqrt{\mu\varepsilon}} \tag{2.43}$$

which is directly depend on material properties and wavelength λ is given as follows

$$\lambda = \frac{v_p}{f} \text{ [1].} \tag{2.44}$$

In free space, where the speed of light is $c = 3\times10^8$ m/s, the wave speed is obtained from Eq. (2.45) ,

$$v_p = \frac{\omega}{\beta_0} = \frac{1}{\sqrt{\mu_0\varepsilon_0}} = c \tag{2.45}$$

where β_0 is phase constant for free air [1]. Eq. (2.45) shows that electromagnetic wave propagates in the free space with speed of light.

Plane wave in a conducting medium

When a plane wave is travelling in a conducting medium with conductivity σ (lossy medium), the wave equation for electric field $\overline{E}$ is given as

$$\nabla^2 \overline{E} + \omega^2 \mu\varepsilon \,(1 - j\frac{\sigma}{\omega\varepsilon})\,\overline{E} = 0 \tag{2.46}$$

in this case, the propagation constant is a complex value and is define as

$$\gamma = \alpha + j\beta = j\omega\sqrt{\mu\varepsilon}\sqrt{1 - j\frac{\sigma}{\omega\varepsilon}} \text{ [1].} \tag{2.47}$$

If again we assume that electric field is uniform in x and y directions and only has the x component then equation (2.46) is reduce to

$$\frac{\partial^2 E_x}{\partial z^2} - \gamma^2 E_x = 0 \tag{2.48}$$

and the solution for such an equation can be written

$$E_x(z) = E^+ e^{-\gamma z} + E^- e^{\gamma z} \text{ [2].} \tag{2.49}$$

The first term of equation, that represents the $+z$ direction of the wave travelling, has a propagation factor of $e^{-\gamma z}$ which is explained as follows

$$e^{-\gamma z} = e^{-\alpha z} e^{-j\beta z} = e^{-\alpha z} \cos(\omega t - \beta z) \text{ [1].} \tag{2.50}$$

The time domain part of equation states that, the travelling wave has phase velocity $v_p = \omega / \beta$, wavelength $\lambda = 2\pi / \beta$ and also an exponential damping factor. Damping factor $e^{-\alpha z}$ states that, when the wave propagates in lossy medium the rate of decay with distance is given by attenuation constant (α).

Similar as loss-less case, the magnetic field equation can be obtained as follows

$$H_y = \frac{1}{\eta}(E^+ e^{\gamma z} - E^- e^{\gamma z}) \tag{2.51}$$

where $\eta = j\omega\mu / \gamma$ is wave impedance.

2.2. Antenna Theory

After discussing about plane waves and propagation of fields in different medium, now we will consider the system which radiates the electromagnetic fields effectively. An antenna, as a fundamental part of a radio system, is a device that transmits and receives the electromagnetic waves. In a communication system antenna operates as a device which converts a guided electromagnetic wave (a wave existing in a transmission line) to a plane wave propagating in free-space. So one side of antenna is an electronic circuit (i.e. transmission line and voltage source) and the other side is free-space. Most antennas are resonant device which works efficiently over a narrow frequency band. This section provides an overview on the antenna fundamentals.

2.2.1. Radiation mechanism

Antenna, as a device at the end of the radiating system, converts the electromagnetic wave to a plane wave propagating in the free-space [2]. Radiation mechanism may better be understood by considering the motion of charges in a wire. Fig 2.1 shows a circular conductive wire which is aligned with Z axis, with length (l), cross-section area of (A) and volume (V). If we assume that the electric volume charge density q_v is distributed in wire uniformly, then the current density J_z over the cross-section of wire is

$$J_z = q_v v_z \tag{2.52}$$

where v_z is uniform velocity of total charge Q moving in volume V [5]. And, in the case of an ideal conductor, where q_s is the surface charge density, the current density on the surface of the wire is given by

$$J_s = q_s v_z \text{ [5].} \tag{2.53}$$

Now, if we suppose that the wire is very thin (ideally zero diameters), the current equation in the wire can be written as

$$I_z = q_l v_z \tag{2.54}$$

where q_l is charge per unit length [5]. Current in Eq. (2.54) is assumed to be time-varying, so derivative of the current is represented by

$$\frac{dI_z}{dt} = q_l \frac{dv_z}{dt} = q_l a_z \tag{2.55}$$

where a_z is acceleration and for wire of length l, Eq. (2.55) can be written

$$l\frac{dI_z}{dt} = l q_l a_z \text{ [5].} \tag{2.56}$$

Eq (2.56) as a basic radiation equation implies that the radiation is produced by accelerated charge or time-varying current. We usually focus on current in case of steady-state harmonic variation and, for transient fields we focus on the charge [4]. The charge acceleration cannot be created if only charge is moving in a straight wire with a uniform velocity, therefore the wire should be curved, bended, discontinued or terminated to create the charge acceleration which causes the radiation. However the charge acceleration can be created if charge is oscillating in a time-motion even if the wire is straight [5].

Fig. 2.2 explains how an actual antenna operates. The picture shows an antenna driven by two-conductor transmission line which is connected to a voltage source. When the source is applied, electric field is created between the conductors. Associated with the electric field, are the electric lines of force which are tangent to the electric field and operate on free electrons of each conductor and force them to be displaced [5]. Movement of charges produce the current and current creates the magnetic field intensity. Since the voltage source is sinusoidal, electric field between two conductors of transmission line is also sinusoidal with same period. The available time-varying electric and magnetic fields, create the electromagnetic wave which propagates along the transmission line and forms the free-space wave at the end of the antenna [5]. In simple words we can say, transmitting antenna is a region where the guided wave is transferred to free-space wave, and vice versa about receiver antenna, that converts the free-space wave to a guided wave [4].

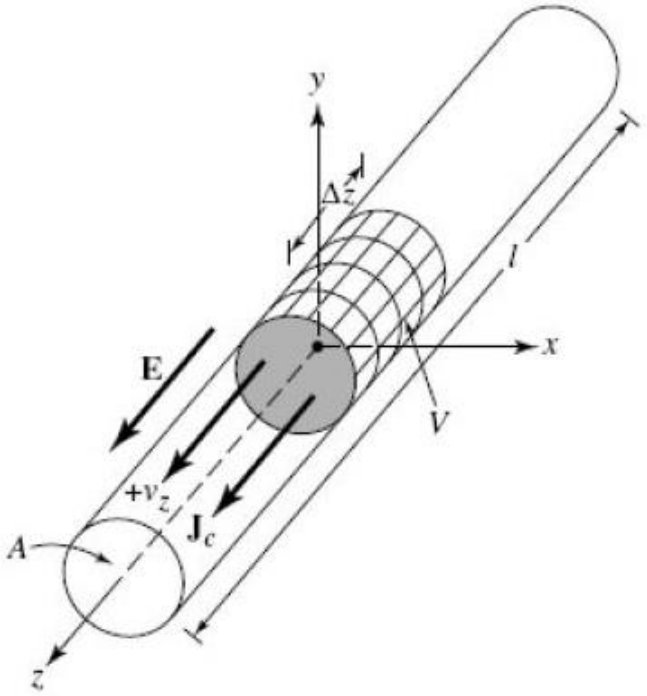

Fig 2.1. Conductive cylinder with charge uniformly distributed in circle cross [5].

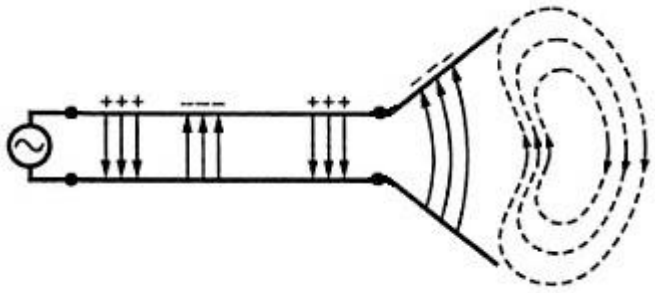

Fig. 2.2. Creation of a free-space electromagnetic wave by an antenna [4].

2.2.2. Antenna parameters

Radiation pattern

Radiation pattern of an antenna is a graphical representation which shows the radiation (far-field) properties of antenna as a function of space coordinates. It describes how the antenna radiates the energy out into the space or how it receives the energy from space. A perfect dipole antenna is a good example to understand the plane patterns. Fig 2.3, shows a perfect dipole formed with two thin wires oriented vertically along the z-axis. The fields radiated from the antenna over the surface of a sphere are represented in picture (a). The plane containing electric field vector is defined as E -plane and the plane containing the magnetic-field is called H -plane. Picture (b) and (c) show the polar pattern of E and H planes. Finally, picture (d) shows the 3D pattern of antenna which looks like a donut or a bagel with the antenna sitting in the hole and radiating energy outward. [6]

Radiation pattern of an antenna can be included the lobes (Fig 2.4) which is classified into main lobe, side lobe, minor lobe and back lobe. The main lobe of a radiation pattern shows the direction of maximum radiation and minor lobes can be any lobe except a major lobe. The side lobe is the lobe adjacent to the main lobe and the back lobe is the radiation lobe exactly in opposite side of main lobe. The half power beam width (HPBW) is one significant concept which is given by antenna radiation pattern. HPBW is defined as the angular distance between the two identical points on either side of the peak. [6]

Field Regions

The surrounding space of an antenna is divided into three field regions, reactive near-field region, radiating near-field region and far-field region. These three spherical field regions represent different operational principles of electromagnetic fields. The boundary separations of these regions are not unique, although different criteria are commonly used to identify the regions. As it is shown in Fig 2.5, the closest area to the antenna is reactive near-field where the reactive part of the field is the most dominant.

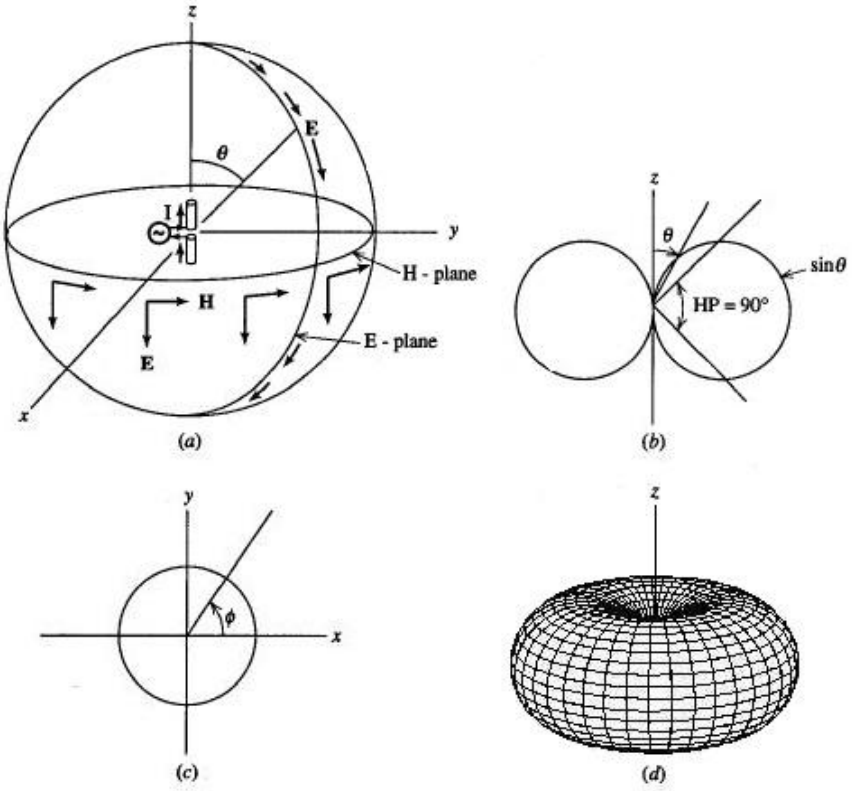

Fig 2.3. Radiation pattern of an ideal dipole antenna. (a) Field components. (b) Polar pattern of E - plane. (c) polar pattern of H - plane. (d) 3D plot of radiation pattern. [6]

The radiation capability of antenna in this region is week. For most of antennas, the outer boundary of this region can be reached at distance $R < 0.62\sqrt{l^3/\lambda}$ from the antenna surface. Here l is the largest dimension of antenna and λ refers to the wavelength of signal. The area between reactive near-field region and far field region is known as radiating near-field or Fresnell region. This region does not exist for those antennas whose maximum dimension is smaller than wavelength. Reactive part of electromagnetic field is not more dominant at this region and field has propagation properties. The inner and outer boundaries for this region is defined as follows

$$0.62\sqrt{\frac{l^3}{\lambda}} < R < \frac{2l^2}{\lambda}. \tag{2.57}$$

The Far-Field region is the outermost region which is also called Frauenhofer region. Far-field region is the region of the field that the radiated wave is well approximated as a plane wave. This region can exist at the distance greater than $2l^2/\lambda$ from antenna surface and l refers maximum dimension of antenna. [5]

Directivity, gain and efficiency

One important parameter for antenna is that how much it can focus the energy towards particular direction in preference to radiation in other direction [6]. This characteristic of antenna is known as directivity and is determined by the shape of antenna and current

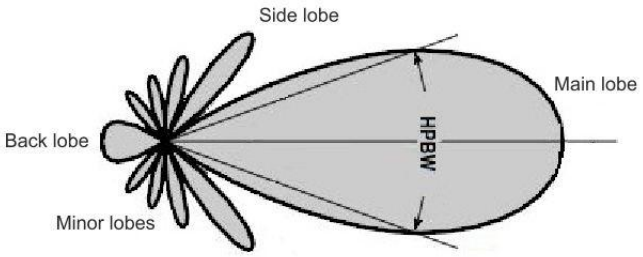

Fig 2.4. Radiation lobes of an antenna [4].

flowing through it. Directivity defines as the ratio of the radiation intensity in a given direction to its average value over all directions,

$$D = \frac{U}{U_0} \text{ [5].} \tag{2.58}$$

Since, the average radiation intensity U_0 equals to the total power radiated by antenna divided by 4π the Eq. (2.58) can be written as

$$D = \frac{4\pi U}{P_{rad}} \text{ [6].} \tag{2.59}$$

When no specific direction is defined, direction of maximum radiation intensity (peak) is intended, so maximum directivity is given by

$$D_{\max} = \frac{U_{\max}}{U_0} = \frac{4\pi U_{\max}}{P_{rad}} \text{ [6].} \tag{2.60}$$

Eq.(2.60) shows that the directivity of an isotropic antenna is equal to unit since the radiation intensity U has maximum value which is equal to its average value ($U_{\max} = U_0$). However, an actual antenna has maximum radiation intensity in the direction of $U_{\max} = D\,U_{ave}$ and the average radiation intensity in direction of $U_{ave} = P/4\pi$. About actual antenna, if we direct the radiated power P in a specific dir-

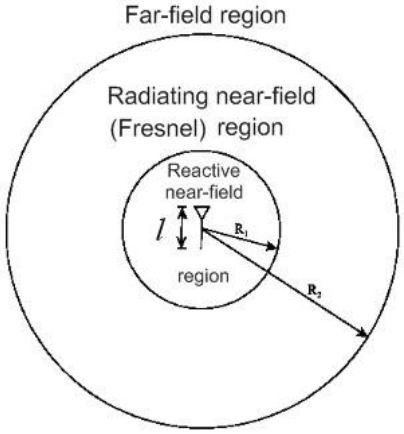

$$R_1 = 0.62\sqrt{l^3/\lambda}$$
$$R_2 = 2l^2/\lambda$$

Fig 2.5. Antenna field regions.

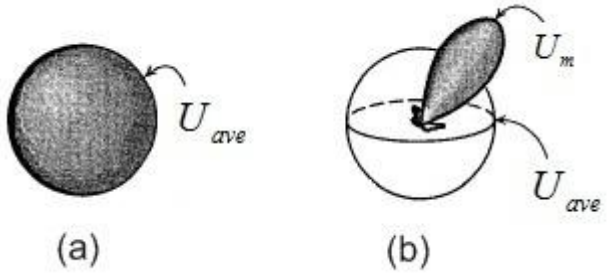

Fig 2.6. Directivity. (a) Isotropic distribution of radiation intensity. (b) Radiation intensity of an actual antenna [6].

ection, the radiation intensity can increase in that direction by using a factor of D over what it would be in case of the same isotropic radiation. Fig 2.6 shows the intensity distribution of an isotropic antenna compare to an actual one. [6]

Gain is the other useful parameter of antenna which describes the antenna's performance. When we use an antenna in a communication system (i.e. as transmitter antenna) we are interested to know how efficient the antenna transfers the available power from its input terminal to radiated power [6]. Gain is the parameter which shows this efficiency of antenna as well as its directional properties. Gain of an antenna is defined as follows

$$G(\theta,\phi) = \frac{4\pi U(\theta,\phi)}{P_{in}} \tag{2.61}$$

where $U(\theta,\phi)$ is the radiation intensity in a given direction and P_{in} is the total power accepted by antenna from input [6]. Similar to directivity, when direction is not specified, gain can be considered in direction of maximum radiation and if the gain value is not given as function of θ and ϕ it can be assumed as maximum gain,

$$G = \frac{4\pi U_{\max}}{P_{in}} \text{ [6].} \tag{2.62}$$

Comparing Eq.(2.60) and (2.62), shows that the different between these two equations is only the power value. By defining the radiation efficiency factor e_r,

$$e_r = \frac{P}{P_{in}} \tag{2.63}$$

the relation between gain and directivity factor is given by

$$G = e_r D \text{ [6].} \tag{2.64}$$

Eq. (2.64) states that the maximum gain of an antenna is proportional to both radiation efficiency and directional characteristic of an antenna.

Input impedance

The impedance presented by an antenna to a transmission line is defined as the ratio of the voltage to current at the feeding point of antenna without load connection. Impedance of an antenna which is connected to terminal of transmission line, is given by

$$Z_a = R_a + jX_a \tag{2.65}$$

Where X_a is antenna reactance and R_a is antenna resistance and it is defined

$$R_a = R_r + R_l \tag{2.66}$$

R_r and R_l refer to radiating power losses and ohmic losses of antenna respectively. The ideal case would be that the whole amount of power coming from generator through transmission line is converted to the radiated power by antenna, but in practice part of power will be reflected back towards the transmission line because of antenna impedance mismatch. This is reason why the impedance matching between antenna and transmission line is preferred. The reflection coefficient Γ is a term that describes how well the energy transfers between antenna and transmission line is, and it defines the relation of the returning voltage wave to the incident voltage wave,

$$\Gamma = \frac{V_0^-}{V_0^+} = \frac{Z_a - Z_0}{Z_a + Z_0} \tag{2.67}$$

where V_0^- is reflected voltage wave, V_0^+ is incident voltage wave and Z_0 refers transmission line impedance. The closer the impedance Z_a and Z_0 .are the closer to zero the reflection coefficient gets and more power will transfer to antenna. The other relevant parameter to impedance matching is return loss which measures the dissimilarity between the impedance in transmission line and antenna. Return loss is calculated from reflection coefficient and is given in decibel

$$RL = -20\log|\Gamma| \ \ dB \tag{2.68}$$

In case of no reflection, the return loss convergence to infinity while its value is zero in full reflection and no energy will transfer to antenna. [7]

Polarization

Polarization of an antenna is defined as the polarization of the electromagnetic wave radiated by antenna in a given direction. Polarization explains the way that an electromagnetic plane wave, which is included the perpendicular electric and magnetic field vectors, propagates at a certain time to a certain direction [6]. Both electric and magnetic field vectors have their own trace of polarization that can be considered, but since magnetic field is perpendicular to electric field, polarization of wave is usually described by electric field polarization. Therefore, more precise definition of

polarization is orientation of the electric field of an electromagnetic wave [6]. Polarization is classified into three different types which are linear, circular and elliptical polarization. As it is illustrated in Fig 2.7, electric field is represented in term of two orthogonal components in X and Y direction and Z axis represents the time and direction of propagation for plane wave. In linear polarization, the strength and length of field components are constant and only direction alternates, while in circular polarization amplitude of two field components are equal but the phase has shifted 90°. When both amplitude and phase of field component vary, the polarization is known as elliptical.

2.2.3. Antenna in communication systems

It is important to consider the antenna in their primary application area of communication link where the antenna plays important role. Simplest form of a communication link can be made by one antenna as transmitter and the other antenna as receiver which are connected through channel (Fig 2.8). Here, we mostly discuss about basic relationship of power calculation in communication link, since the further detail related to communication link is not so relevant to scope of this study.

Power in receiver antenna is summation of the incident power density over whole area of receiver antenna where is called effective aperture. How well an antenna converts this incident power to available power at its terminal, is something that depends on antenna parameters such as directivity and polarization and also the type of antenna that has been used. The effective aperture can be define as follows [6]

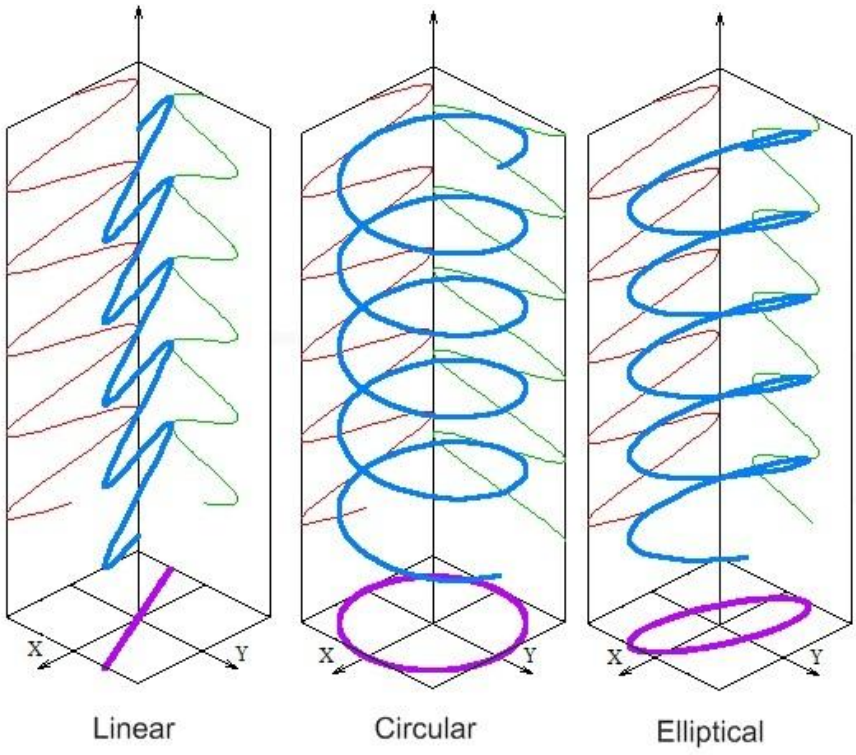

Fig 2.7. Different polarization forms of an electric field [8].

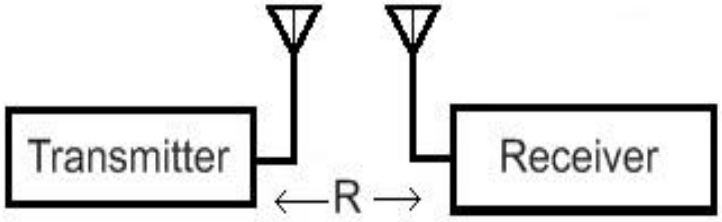

Fig 2.8. Communication link between transmitter and receiver at distance R from each other.

$$A_e = e_r A_{em} \tag{2.69}$$

where e_r refers the radiation efficiency and A_{em} is maximum effective aperture that is defined in lossless case. So the available power at receiver antenna is given by

$$P_A = S\ A_e \tag{2.70}$$

where S is power density incident on the receiver antenna [6]. Eq. (2.69) states that the power received by receiving antenna is reduce to the fraction e_r of what it would be if the antenna were lossless. Eq. (2.70) implies that the receiver antenna act to convert the incident power density to power delivered to the load. It is good to note that the relationships which are developed for receiver antenna they all can be applied to transmitter antenna as well.

Now we are ready to describe the power transfer in the communication link of Fig 2.8. According the equations are derived in the [6], the received power P_r by receiver antenna which is placed in distance R from transmission antenna is given as

$$P_r = P_t \frac{G_t G_r \lambda^2}{(4\pi R)^2} \tag{2.71}$$

where P_t is transmitted power by transmitter antenna, G_t and G_r are the power gain of transmitter antenna and receiver antenna respectively and λ is wavelength. The Eq. (2.71) which is called the Friis's equation is very useful to calculate the signal power level between transmitter and receiver antenna. If there is a different between the estimated power by Friis formula and the actual received power in receiver, that might be because of mismatch between antennas (transmitter and receiver) with the connected transmission lines or not having the identical polarization in both transmitter and receiver antenna. [6]

2.3. RFID System

Radio frequency identification (RFID) was developed around the Second World War This technology that provides wireless object identification has become very popular in our life. RFID is a system developed for short-range radio technology used to communicate mainly the digital information between a stationary location and several movable objects.

The main reason for developing such a technology is the capability to identify and track the movement of the products through the supply chain. This is important for retailers because, it reduces the likelihood of items being out-of-stock. For more than forty years, the barcode system has been used for product tracking in supply chains, but the RFID systems are more robust since they offer a possible fast, reliable and real time method for identifying the objects. The radio frequency based identification does not need the line-of-sight like barcode systems, and this ability provides a significant flexibility to the RFID system. Reading distance of RFID system is also better than the barcode system. It starts from few centimetres to around ten meters. RFID tags are able to carry more information than using the barcode systems, since they use IC which stores more information in its memory and it can be updated in real-time. There are many other advantages for RFID systems, but manufacturing cost which is usually more expensive than the barcode system and also implementation issues, are the main limitation factors for RFID systems.

The radio frequency part of RFID system is the communication between tags and readers. In a typical passive RFID system, each individual object is labelled with a tag which consists of an antenna and integrated circuit (IC) which has the product information inside memory. The reader sends a signal to make the tag active and then the information stored inside the tag is backscattered to reader and is passed to a host computer for processing.

This section introduces the RFID fundamentals such as system configuration, classification and standardization. The RFID systems component and block diagram of system are first introduced, then the system classification and standardization will be addressed. In the next chapter, more detail about the design of a RFID tag is considered.

2.3.1. System configuration and components

An RFID system consists of the tag, reader and host computer, shown in Fig 2.9. The reader communicates with the tag by using RF signals to get the information stored on tag. The communication between the reader and the tag is directed by an application host and the results are reported to the host.

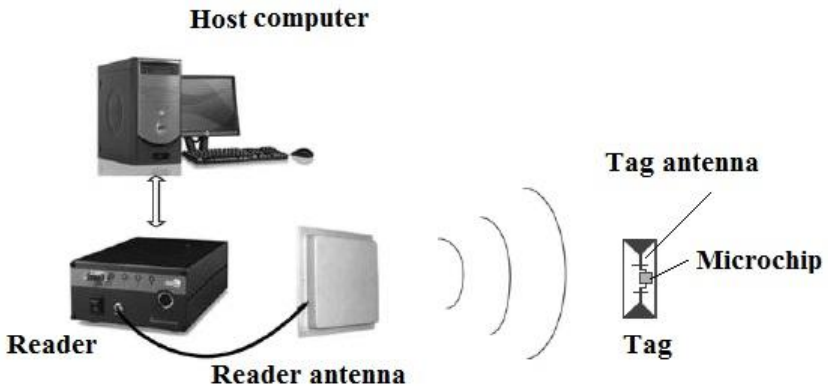

Fig 2.9. RFID system configuration [11].

An RFID tag is the device that stores and backscatters the information to a reader with the help of EM waves (contactless). The family of tags that do not use the IC are called chip-less tags. A common chip tag implementation consists of two main components, a small silicon IC, which has a unique identification (UID) number and stores the data and implements the tag's functionality, and an antenna that is used for RF communication with reader. These two components will be attached to a dielectric substrate material and form an RFID tag. The size of a tag can be very small, due to the use of a tiny chip (potentially less than half a millimetre). Moreover, the size of the antenna is very small, which might only be a loop with less than one centimetre diameter. Fig 2.10 shows some RFID tags of different sizes and shapes. Since tags can be quite small and thin, they can be easily embedded into packaging, plastics cards, tickets, and also can be used for book and cloth labelling. RFID tags can be divided to three categories according their energy source: passive, semi passive and active tags. More detail will be provided in the next section.

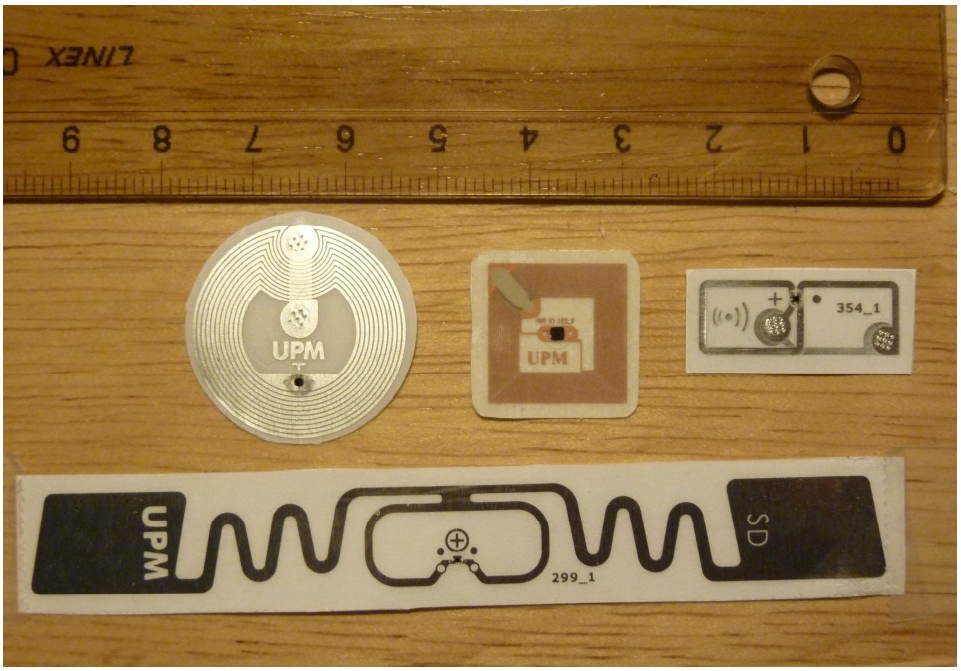

Fig 2.10. RFID tags.

Reader or interrogator, as the central nervous system of RFID hardware, is a device that read the data from compatible tag and also writes the data to compatible tag. Thus, reader can work as a writer as well, and process of writing to the tag by reader is called creating the tag [11]. Creating a tag, which can be uniquely associating the tag with an object, is known as commissioning the tag and similarly, decommissioning a tag is disassociating the tag from a tagged object [11]. A reader is composed by different parts like microprocessor, controller, memory, power supply and the main part for communication with tag, which is antenna. The reader antenna works as a transmitter and receiver antenna together and for this purpose it uses mono-static radar configuration [9]. Similar to every other transmitter, reader as a transmitter must have the following features [9]:

Accuracy: It needs to be accurate in modulation of the carrier frequency with desirable baseband signal and maintain the carrier at desired frequency.

Efficiency: an undistorted signal at the desired output power and without wasting too much DC power should be provide by transmitter.

Low spurious radiation: delivered signal by the transmitter needs to be clean and spur-free with respect to amount of available DC power.

Flexibility: for power saving purpose, it should turn off when not in use and turn back on quickly if it is needed and does not make a large interfering signal in this process.

as receiver, it should provide [9]:

Sensitivity: thermal noise can be considered as the ultimate limit of radio sensitivity and a good RFID radio must receive and interpret a very small signal successfully.

Selectivity: in the presence of every other powerful interferer, it should be able to detect the tag signal.

Dynamic range: same reader must receive and interpret the signals from a tag in different distance from antenna.

Flexibility: in passive RFID protocols, the transmitter sends a signal which is amplitude modulated and then it transmits the CW signal when it is waiting the response from the tag. Receiver should recover very fast from any disturbance caused by the portion of modulated signal that leaks into it, to be able to detect the small tag response.

Other component of an RFID system is application host. The host computer system is an all-encompassing term for the hardware and software components that are separate from RFID hardware such as the reader, reader antenna and tag. The host computer system mainly consists of: the edge interface/system, middleware, enterprise back-end interface. [11]

Combination of the basic components of an RFID system is essentially the same for all application and variation of RFID systems. Readers are usually placed at strategic

entry places where they should collect product-related information. All the objects that should be identified are labelled with RFID tags. The only things that will be different from application to application are the type of the tags and data stored on the tags. [13]

2.3.2. Classification of RFID systems

RFID system can be classified by their tag's energy source, operation principles, frequency bands and tag memory types.

Active, semi-passive and passive

Denoting tag energy sources and how is powering up for RFID tags, system is categorized into three groups: Active, semi-passive and passive.

In active RFID system, tag has an internal energy source such as on-board battery. It uses its on-board power supply for supporting IC operation and data transmitting to reader. Since tag can wake the IC up by its internal energy source, it does not need to wait for reader to start the communication and tag always communicates first. Therefore, an active tag can broadcast its data to the environment around it, even in the absence of reader antenna. These type of active tags are known as transmitters. Because of energy saving issues and also reducing RF noise, there is another type of active tags which is in sleep state as long as there is a wake-up request from reader. These type of active tags are called transmitter/receiver. [9]

The semi-passive tags use internal power source for its operation, however it harvest the communication energy from the reader. For this type of a tag, in tag-to-reader communication, reader always communicates first followed by tag. The advantage of a semi-active tag to passive tag is that it does not need the reader's signal to be energized so reading distance is longer compare a passive tag. [9]

A passive tag gets the power for both operation and communication from reader side. It does not have any internal power source and use the power emitted from reader to excite itself and transmit data to reader. So in tag-to-reader communication, reader always starts the communication and presence of the reader is mandatory. A passive tag has simple structure compare to active and semi-passive tags which led to being cheaper and lighter and having more operational life-time. However, shorter read range and requiring higher-power reader are considered as limiting factors for passive tags. [9] [11]

Operation principles

In terms of method of power transferring from reader to tag, RFID systems can be divided to far-field systems and near-field systems. For either of them, the coupling mechanism between reader and tag is different since electromagnetic fields behave differently in each zone.

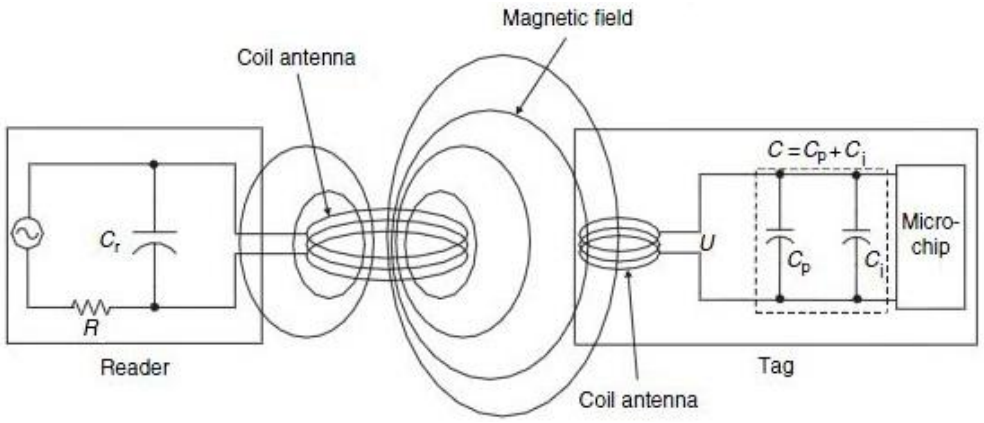

Fig 2.11. Inductive coupling mechanism between reader and tag [14]

In near-field RFID system the power transfer between the reader and tag can be achieved by inductive coupling or capacitive coupling, however the inductive coupling is more commonly used. Fig 2.11 shows the mechanism of the inductive coupling. First the reader coil produces a strong magnetic field which induces some currents in the coil of the tag and generates the voltage U in tag's coil. This voltage acts as a power supply for IC (after rectified inside IC) and energizes the IC. Then capacitor C_i which is connected in parallel with tag coil forms a resonant circuit tuned to the transmission frequency of the reader antenna. Voltage U gets the maximum value due to resonance set-up in parallel resonance circuit. In fact, the reader-tag system acts as a magnetic transformer which provides the coupling between the current flowing in the reader and the voltage across the tag. After energizing the IC, IC can execute the reader's commands. The loop antenna can be suitable case for inductive coupling. The capacitive coupling which is also named as electronic coupling occurs when the antennas create and interact with quasi-static electric field. Here reader antenna generates electric fields and the tag antenna is made up of two conductive surfaces lying in a plane (electrodes). When the tag antenna is placed in electric field of reader antenna, the voltage between electrodes increases and acts as power supply voltage for energizing the capacitor. A dipole antenna can be a suitable antenna for capacitive coupling since the electric field dominates the magnetic field. [14]

Far-field RFID systems, operate at UHF and microwave frequency bands. In far-field system, the communication between the reader and tag is realized by backscattering coupling. Fig 2.12 shows the backscattering mechanism. Tag antenna receives the energy which is sent out by reader antenna and part of that energy will be reflected back from tag and detected by reader. The reflected signal can change by varying the impedance mismatch of the tag. In the other words, the variation of tag's load impedance (IC) causes the impedance mismatch which can effect on amplitude of the reflected energy from tag. From variation of the reflected signal, the tag's ID can be encoded by reader. This way of communication is known as backscattering modulation. [10],[11]

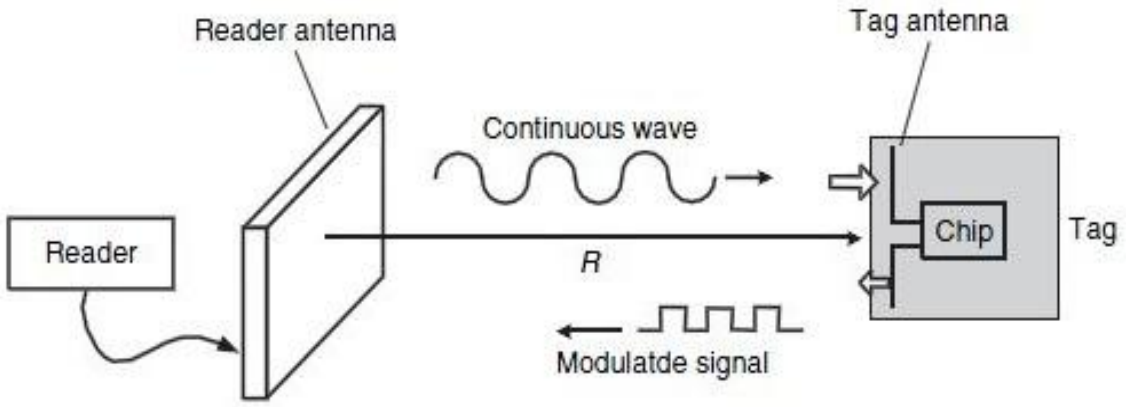

Fig 2.12. Configuration of backscattering coupling between tag and reader [11].

Frequency Bands

Since the RFID system generates and radiates electromagnetic waves, they are classified as radio system. Depending on application, the RFID system frequencies vary from around 100 KHz to over 5 GHz. but the most commonly used frequency bands are the 125/134 KHz, 13.56 MHz, 860 - 960 MHz and 2.4 - 2.45 GHz. The 125/134 KHz operates inside the low-frequency (LF) band and they are usually referred to LF tags and readers. The reader and tag at 13.56 MHz work within the high-frequency (HF) band and are characterized as HF systems. 860 - 960 MHz and 2.4 GHz operate within the ultra-high-frequency band (UHF). 860 - 960 MHz reader and tag are referred as UHF system. The UHF frequency band (860 - 960 MHz) can be divided to Europe region frequency (868 MHz), USA region (915 MHz) and Japan region (952 MHz). [9]

One significant concept related to frequency of the wave is wavelength. Waves travel in vacuum with speed of light $c = 3 \times 10^8$ m/s and wavelength λ is defined as the ratio of the speed of light to the frequency, $\lambda = c / f$ [m]. So varying the frequency range will bring a huge range in wavelength. For instance, wavelength of a wave with frequency 0.3 MHz is about 3000 times longer than a wave with frequency 900 MHz The commonly used wavelength in RFID system is from 2 km to about 12 cm. As a conclusion, we can also classify the RFID system by whether wavelength is comparable to the antenna size or widely larger than the antenna size. If the wavelength is much larger than antenna size, the energy transfer between tag and reader is inductively coupled and most of the available energy of reader antenna is inside a small region near reader antenna. Inside this region, the communication between the tag and antenna is effectively instantaneous and it is difficult to distinguish the transmitted and backscattered signal. When the antenna size is comparable to the wavelength, the communication between the reader and tag is done by backscatter coupling. Due to the far-field nature of the communication mechanism, transmitting the wave from reader antenna and returning back a distinct wave by the tag, take more time compare to the inductive coupling. [9]

Tag memory

The quantity of data that can be stored in a RFID tag depends on the memory size of the tag. It can be from few bits to several kilobytes. There are usually three different types of tag memories: read only, write once read many (WORM) and read and write. Data is set in read-only tags during manufacturing of tag and it provides limited flexibility to the system to updates the specific data inside the tag. About WORM tags, data will be set by tag owner sometimes after tags have been manufactured. So when the data is set, it cannot be changed and only can be read. Read/write tags allow the user to set and reset the data content of the tag. Ability of writing data on the tag provides significant flexibility to RFID systems. [13]

2.3.3. Standardization for applications

RFID system standards are developed to explain the format and content of the codes placed into the tags, the communication protocols and the frequencies that will be used by the tags and readers, as well as the security issues [12]. At the moment, RFID systems can use a few standards that no one has been universally accepted and competing the standards have been one of the difficulties for RFID systems [14]. International Organisation of Standardisation (ISO), EPC-global Inc, European Telecommunications Standards Institute (ETSI) and Federal Communications Commission (FCC) are some of the standards which are involved in the development and definition of RFID systems. Here we introduce parts of the ISO and EPC family standards.

EPC (Electronic Product Code) has proposed by Auto-ID center and its goal is moving from established standards for barcodes to a new EPC. EPC tag classes are divided to five different classes that each of them has different data structure and operation. They are described as follows [9]

- Class 0 is for read only passive tags,
- Class 1 refers one-time writable and read many (WORM) passive tags with minimum 96 bits,
- Class 2 (Gen 2) is for read and writable passive tags with minimum 96 bits,
- Class 3 is the read and writable for semi-passive tags,
- Class 4 is also read and writable but for active tags.

The EPC code structure is included a number which is divided into four different parts. The first part of EPC code is header which identifies the EPC's version. The second part is EPC manager or manufacturer of the product. The third part of the code or object class, refers to the exact type of product and the last part is the unique serial number of item.

The International Organization for Standardization (ISO) has developed different

standards for different RFID applications. Some of them are described as follows [14]

ISO Standards for Proximity Cards:

ISO 14443 for proximity cards and ISO 15693 for vicinity cards, use the HF frequency band (13.56 MHz) as its carrier frequency. ISO 14443 offers a maximum read range of few centimetres and mostly is utilized for financial transaction and high secure application. ISO 15693 vicinity cards or Smart Tags, offer a maximum read range of about 70 centimetres from a single antenna.

ISO Standards for RFID Air interface:

The ISO 18000 series is set of standards for item management. It is divided to seven different parts to cover all popular RFID frequency bands including 135 KHz, 13.56 MHz, 860-930 MHz and 2.45 GHz.

18000-Part 3 refers parameters for air interface communications at 13.56 MHz.
18000-Part 6 defines specifications for air interface communications at 860-930 MHz.

ISO Standards for Animal Identification:

ISO 11748 and 11785 are standards for animal Identification.

Chapter 3

3. Passive UHF RFID Tag Antenna

In the last section of the previous chapter, there was a general discussion about the RFID systems. Since the main goal of this thesis is optimizing the tag antenna design to improve the performance of the tag in close proximity applications, it is important to discuss about the tag design in more detail. There are many different approaches to the antenna design. In this thesis, most of the information about design of passive UHF tags is gathered from the available literature however, part of it is based on a learning process to UHF RFID tag design. There are many different factors which play significant roles in the design of a cost efficient and reliable tag product. These are for example designer's experience, sufficient information about application which the tag is going to be used for, using the professional design tools and measurement equipment. However, there are always a trade-offs in design process. This means that improvement in some of the properties may cause losing part of the other properties.

This chapter presents the passive UHF RFID system and takes a closer look at tag antenna design. In order to discuss about the tag antenna design, the operational principles of passive UHF RFID system are first described. Then some of the design requirements and considerations are discussed with respect to application, and also some design methods for improving the antenna performance are given. In the third section of this chapter, a general design process is described and finally an example design that is used in close coupling study is explained.

3.1. The Structure and Operational Principle

As it is mentioned in Section 2.3.2, communication between tag and reader antenna in long range passive UHF RFID system is done by backscattering modulation method. In the radio link between the tag and the reader, the forward link refers to the process of carrying commands and power from the reader to the tag, whereas the communication from tag to reader is referred as the reverse link that carries the reply. The

communication between the reader and tag is half-duplex, which means that when the reader is transmitting, the tag is listening and vice versa.

According EPCglobal UHF Class-1 Gen-2 standard [15], the tag antennas use amplitude shift keying (ASK) and/or phase shift keying (PSK) modulation techniques for communication with the reader. The tag encodes the backscattered data as either FM0 baseband or Miller modulation of subcarrier [22].

Fig 3.1 shows the block diagram of a passive backscatter RFID system. The communication starts when the reader emits continuous wave (power) to activate the tag. The continuous wave is followed by a command, typically a query command [20]. After the query command, reader sends a continuous wave which is then modulated and backscattered by the tag. When the tag has obtained enough energy to run the IC, then it sends the data back to the reader using its own modulation. The modulation of the scattering from the tag is realized by switching the input impedance of the IC between two different states Z_{C0} and Z_{C1} according to the EPC [20]. These two impedance states refer to the matched and mismatched impedance states of the chip, so in the case of poor matching almost all incident power to the tag antenna will be backscattered to the reader. But in well-matched case (tag antenna is conjugate matched to the IC), the power is transferred from the tag to the chip and only a fraction of transmitted power is backscattered [20], this is the reason why the received backscattered signal from the tag is much smaller than the transmitted signal. Since, at each impedance state tag presents a certain radar cross section (RCS), this provides a significant difference in the backscattered signal. As it is illustrated in Fig 3.2, the baseband symbols change between low and high power stage and coding is done by a way in which, the binary 1 is a long full-power interval followed by a short power-off pulls and binary 0 is a shorter full-power interval followed by same power-off pulse. The reason why the binary 0 also start with a full-power interval is that if the data is containing bits of zero for long time, the tag will get turned off. Also, using equal low and high pulses for binary 0 ensures that at least half of the maximum power is delivered to the tag even when the transmitted data contains long string of zeros.

According EPC class1 Gen2 protocol [15], reader can use ASK modulation technique which is depicted in Fig 3.2 as well. From the figure we can also see that the

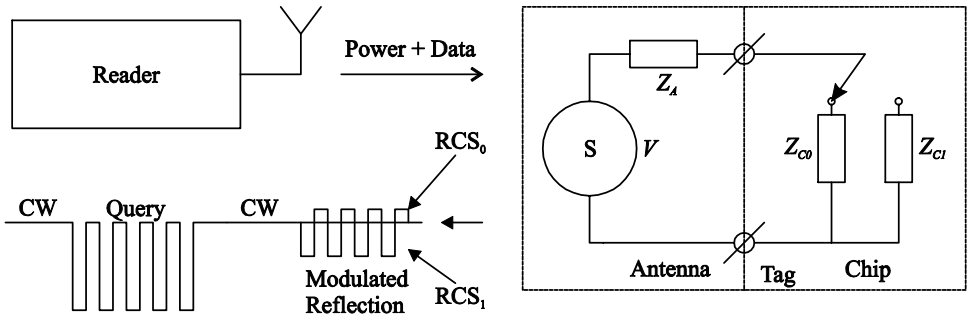

Fig 3.1. Passive backscattered UHF RFID system. Picture edited from [19]

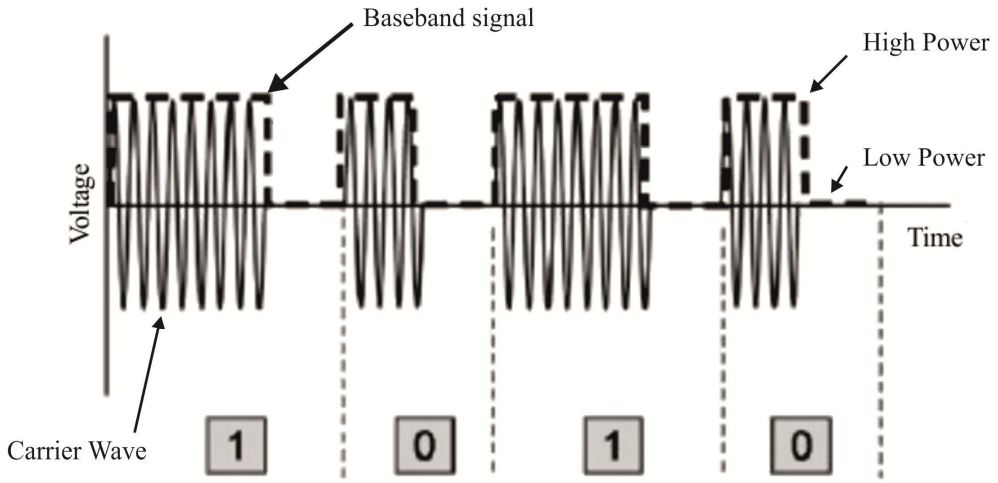

Fig 3.2. PIE with ASK modulation of carrier wave. Picture edited from [9].

amplitude of the carrier oscillation is switched between two states of encoded baseband signal so that the CW envelope is altered according to the amplitude of the baseband signal. Single-sideband (SSB-ASK), double-sideband (DSB-ASK) and phase-reverse (PR-ASK) are the ASK techniques which can be used by reader for modulation. [19]

3.2. Design Considerations

The performance of an antenna was described by number of antenna's parameter in Section 2.2.2. From the design point of view, by changing one of those parameters some others will be affected. Therefore, finding balance and realistic performance target is one of the most difficult challenges in the design. However, in UHF tag design there are some common highlight issues which should be considered during the design work. One of them is size and shape of tag antenna. Most of the far-field UHF RFID tag antennas are modified dipoles, since dipole antennas harvest the energy from all direction and there are more methods for matching and size reduction of dipoles. They have to be modified because an unmodified half-wave dipole is too large to be used in UHF RFID applications and its reactance is too small to be matched to the tag IC. The other significant issue is matching and power transfer between tag antenna and chip. Maximizing the read distance and the parameters which affect the read distance are also important in design.

3.2.1. Matching techniques

The tag antenna transfers power to the chip (IC) and this power transfer should be maximized because the transmitted power from the reader antenna is limited and also the IC sensitivity is finite. The power P_r that tag antenna receives from the reader antenna, can only be delivered to the tag IC in case of maximum power transfer and that is when the tag antenna impedance ($Z_A = R_A + jX_A$) is conjugate-matched to the IC

impedance ($Z_{chip} = R_{chip} + jX_{chip}$). In this section, some useful matching techniques are introduced for dipole antennas.

T-Match is one of the most commonly used matching networks [18]. Fig 3.3 shows a typical dipole tag with T-matching design and its equivalent circuit. In fact T-match circuit acts as a transformer that conjugates matches the antenna input impedance to the chip (IC) impedance through parameter α. The tag consists of a dipole with length of l and the width of w which is connected to a short-circuit stub of length $a \le l$. The tag's IC is also connected to the short-circuit stub which is kept at a distance b from the main radiating element. The input impedance Z_{in} at the point where the source is connected is given by

$$Z_{in} = \frac{2Z_t(1+\alpha)^2 Z_A}{2Z_t + (1+\alpha)^2 Z_A} \tag{3.1}$$

where $Z_t = jZ_0 \tan(ka/2)$ is the input impedance of short-circuit stub, $Z_0 \cong 276\log_{10}(b/\sqrt{r_e r_e'})$ is the characteristic impedance, $r_e = 0.25w$ and $r_e' = 8.25w'$ are the equivalent radii of the dipole and the matching stub, respectively, Z_A is the tag antenna input impedance without T-matching section and $\alpha = \ln(b/r_e')/\ln(b/r_e)$ is the current division factor between the conductors. By adjusting the geometrical parameters a, b, w and w', the antenna impedance can be matched to the complex chip impedance, Z_{chip}. Use of T-match in impedance matching has been discussed in many publications [18], [20], [21] and it is understood that sometimes even with small value of a and b, high value of input resistance can be reached. In this particular case, a single T-match is not enough for conjugate matching and further modification like multiple T-matching can be used. [18]

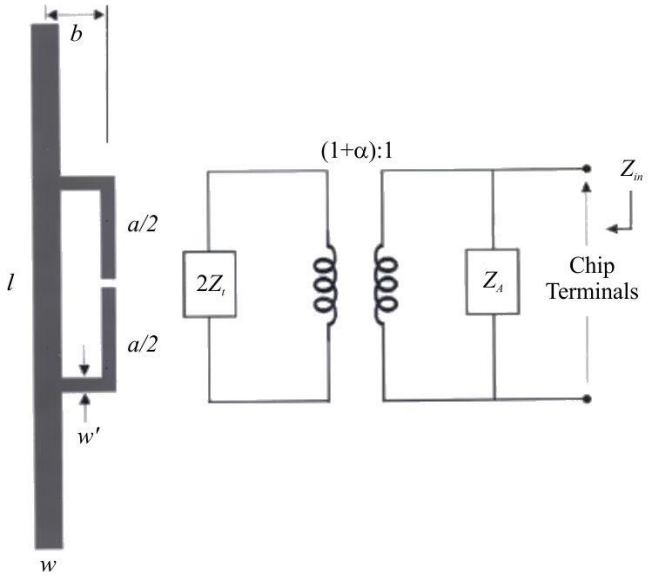

Fig 3.3. T-matching configuration and equivalent circuit model for a planar dipole antenna. Picture edited from [18].

Inductively coupled loop can be used as other method for tag antenna matching [18]. As illustrated in Fig 3.4, the radiating dipole antenna is fed by inductively coupled small loop which is kept in close proximity to the radiating part. The IC is directly connected to the loop terminal. This configuration adds an equivalent inductance in the antenna, and strength of the coupling and the added reactance are controlled by the distance between the radiating part and the loop and also the shape factor of the loop. The inductive coupling can be modelled by a transformer, and the input impedance seen at the loop's terminal is given by

$$Z_{in} = Z_{loop} + \frac{(2\pi fM)^2}{Z_A} \tag{3.2}$$

where, $Z_{loop} = j2\pi fL_{loop}$ is the loops input impedance. No matter if dipole is at resonance or not, the total input reactance depends only on the loop inductance, L_{loop} whereas the resistance is related to the transformer mutual inductance, M ,

$$R_{in}(f_0) = (2\pi f_0 M)^2 / R_A(f_0) \tag{3.3}$$

$$X_{in}(f_0) = 2\pi f_0 L_{loop}\,. \tag{3.4}$$

The mutual coupling and the total input resistance are dependent on both the loop shape and the dipole-loop distance, while the reactance, L_{loop} , is mainly affected only by the loop aspect ratio. The design step involves choosing the loop shape and size for cancelling the chip capacitive reactance and then properly choosing the loop-dipole distance, d , to match the chip's resistance. [18]

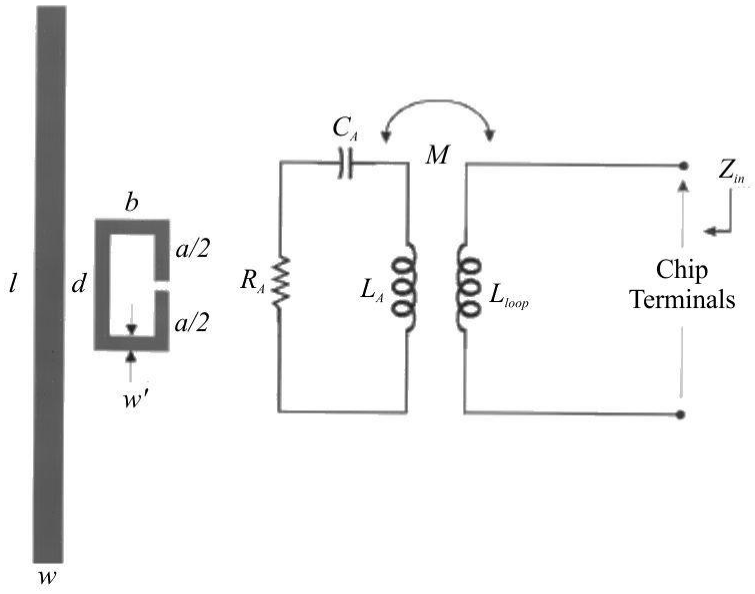

Fig 3.4. Inductively coupled configuration and equivalent circuit of dipole antenna. Picture edited from [18].

Both antenna and chip impedances are function of frequency. In addition, chip impedance is a function of power absorbed. This is the reason why the complex conjugate matching only happens at a single frequency. Therefore, for a wideband design, the other matching techniques are more suitable. [20]

3.2.2. Size reduction

In design process, the size and form of antenna inlay is usually determined according the application specification and it is fixed. In case of using same IC and adjusting the identical and optimal matching condition, the bigger the physical size of tag antenna is the bigger is the reading distance. If the large read distance is the goal of the design, it results into having a large tag antenna [16].

The length of a half-wave dipole antenna in UHF band is about 16 cm in free space. Since, in most of the applications, tag has to be attached onto a small object, some size reduction techniques should be utilized for the design to meet the specification, but still the tag antenna has to have good radiation efficiency. Meander line structure is one of the most commonly used techniques to downsize the tag [18]. This can be done by single or even multiple folding of the radiating part of dipole antenna. Meandering the radiating body of antenna affects the antenna's input impedance. The change of input impedance (because of using size reduction methods) and its effect on matching can be optimized by adjusting the design properties of the matching point. The other example technique for size reduction is called Inverted-F configuration which has been discussed in detail in [18]. In addition, the miniaturization techniques concerning the small antennas has been discussed widely in [45].

3.2.3. Other consideration

Antenna read range is one of the critical requirements in the design which should be considered. Some of the tag or reader antenna's properties, such as transmitting power, antenna gain, operating frequency, radar cross-section (RCS), quality factor, polarization and sensitivity, can be considered as factors that affect the read distance. For instant, Eq. (2.71), Friis equation, demonstrates that read distance is affected by reader and tag antenna's gain. The read range can also be increased by increasing antenna RCS. Radar cross-section σ, which is used to characterize the scattering properties of the tag, depends on a series of parameters such as tag's size, shape, material, surface structure and the used wavelength and other parameters. In case of a good matching condition, the larger the antenna's reflecting surface is the more energy it receives from the reader field. This improves the read distance. [19]

Desired frequency band in design of tag antenna depends on where the tag will be used and what do regulations of that country. A tag antenna with very large bandwidth

covers the entire three frequency bands ETSI, FCC and ARIB. This means the tag is working well as a global product. The bandwidth can be increased by changing the antenna's shape. In addition, using the dual port antenna, as a broadband antenna, can improve the bandwidth [16].

Cost is also one of the issues that should be taken into account in the design of a tag antenna. The antenna structure and materials which are used, affect to the price. Commercially, the typical conductors used for tag design are aluminium, copper and silver ink, and the dielectric material can be flexible polyester or paper. Using the Aluminium is cheaper compared to copper and silver.

Reliability of products is also an important issue. Tag must be reliable device that can sustain variation due to temperature, humidity and mechanical stress, and survive such processes as label insertion, printing and lamination. [19]

3.3. Design Process

Design process starts after defining a business case which usually comes from a customer and marketing department. The design requirements are usually determined by the application which tag is going to be used in. The design work can be done more efficient, when there is more input information available from the client application. Once the application is selected and design requirements have been defined, the materials for tag antenna construction can be determined.

The actual design work usually starts with simulation of the tag antenna which makes the antenna parametric study possible. By simulating the design, optimization of design is performed until the design requirements are met. Tag antennas are usually analyzed with electromagnetic modelling and simulation tools, with method of moments (MoM) for planar design and with finite-element method (FEM) or finite-different time-domain method (FDTD) for complex 3D design [17]. Using a fast electromagnetic analysis tool is efficient for the design work. For this thesis, the antenna's design has been modelled with AutoCAD software and the final layout has been imported to the simulation software, microwave studio CST.

In the next step of the design process, prototype samples are made. To avoid the repetition of making samples for optimization of design, the possible variation in design can be made as a design matrix. After the prototype samples of design matrix become ready, their performance can be measured and the best matrix member can be selected for final measurement. If design requirements are not satisfactory, the design needs further modification and it should go back to the simulation step again. However, if requirements have been met, the design work is done.

After the design, the overall performance of the tag should be evaluated and some tag antenna parameters should be measured. Measurement of many antenna parameters is

difficult due to mismatch between tag antenna impedance and typical impedance of RF measurement equipment (50 Ω or 75 Ω). Theoretical read range, power on tag, transmitted threshold power, radiation pattern and the backscattered signal power are the most common measured quantities in evaluating the tag performance. Theoretical details of these measurements have been described in [20]. In this thesis, the measurement of the mentioned quantities was done using Voyantic Tagformance Lite measurement system. Voyantic Tagformance Lite is a complete measurement solution for evaluating the functionality and performance of EPC Class 1 Gen 2 tags.

3.4. Design Example

Here we focus on an example design which is named Web and it is a Smartrac product. This product has been made to be used in stack application, so tags should have a good performance when they are placed in stack horizontally at top of each other and also each single tag should work well individually. The performance of product should finally meet the UofA application measurement targets. UofA is set of standard application measurement for UHF tags which is defined by University of Arkansas. In UofA tests, there are different types of measurements for single tag performance in free air and on top of the materials like jeans or denim. We will know more about UofA test methodology in chapter 5.

In order to start the design phase, all the possible information about the product should be gathered. This can be done by help of marketing department which is in direct contact with customers and they usually define the required frequency, physical size, the shape of the tag, the surface tag is going to be attached to and many other non-technical data which are very important to be clarified. Based on this information, it is the designer's job to survey if the product, in physical sense, can be made or not. For the Web product the technical specifications are listed in Table 2.

Table 2. Technical specification for Web design.

Operating frequency	902-928 MHz
Resonance frequency in free air	908-912 MHz
Application material	To be used on top of the plastic material
Antenna layout size	50 mm × 30 mm
IC type	Impinj Monza 5
Close coupling performance	Pass the UofA targets

From specification the tag antenna layout size is defined 5 cm by 3 cm. The electrical length of antenna is defined by desired resonant frequency. Unloaded resonance frequency target is based on a careful estimation of how much the tag environment would detune the tag antenna [16]. This estimation mostly comes from experience of

antenna designer and knowledge about the different material detuning effects. The effect of detuning can be compensated by tuning the antenna resonant frequency higher than the target frequency of the application. Since the Web antenna is measured on top of the materials such as jeans and denims, which have very heavy detuning effect, the antenna has to have a large bandwidth to cover the used frequency in case of thinner (small detuning effect) and thicker (big detuning effect) materials. For covering a large bandwidth, the design is done in a way that, the magnitude response of antenna (in simulation and measurement) looks like a band-pass shape which has two resonance peaks. One of the peaks shows the loop resonance frequency and the other one refers the radiator resonant frequency.

The AutoCad software was used to make the antenna layout. Couple of iteration circles of design and redesign might be needed between AutoCad and CST simulator software to find the correct resonant frequencies. Usually frequency tuning can be done by changing the length of radiator element of antenna and loop shape. The proper matching can be achieved by adjusting the loop structure and also the connection point between loop and radiating part which is used as matching point. Fig 3.5 shows the web antenna layout which is composed of three different parts. The loop's structure is made for adjusting the loop's resonant frequency and also for impedance matching. The IC which has been used for this product is Impinj Monza 5 [23]. The chip capacitance is 1.07 pF and its parallel resistance is 1.8 kΩ. IC is connected to the loop terminals and the gap between two terminals was adjusted with respect to the bump separation. The conjugate matching can be achieved by adjusting the width of matching point and also the gap between the loop and radiating part. The radiating part structure is made for adjusting the radiator resonance frequency. The folded shape arms are adjusted to get less current cancellation passing through curves and having a good close coupling performance which is main goal of this product. The amount of metal on antenna surface area will affect RCS and hence the antenna performance and read range. Here the folded arms are designed narrow to get good close coupling performance (by having less capacitive coupling between the antennas). To keep the surface area still large, and have a good read range, the end elements were designed wider.

After preparing the antenna layout, the antenna parameters can be analyzed in simulator CST, software. For simulation purpose, the web design has been simulated by placing the antenna's layout on top of PET substrate material with thickness of 3 mm. Many of the antenna's parameters such as impedance response, efficiency, radiation pattern and theoretical read range can be monitored by using simulator CST. Here, the S_{11} simulation result for the Web is shown in Fig 3.6. The S_{11} graph (which in this case is referred to complex chip impedance) describes some properties of the antenna's design such as quality of matching and resonant frequencies. The magnitude response of

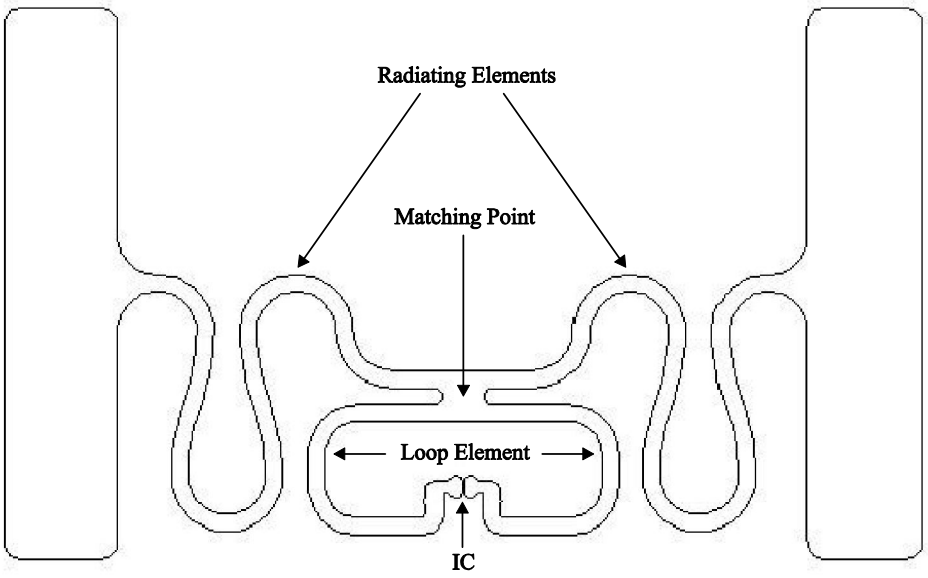

Fig 3.5. The Web antenna's layout.

S_{11} graph shows that in an ideal form, the antenna receives the most energy at 865 MHz and 950 MHz which are loop resonance frequency and radiator resonance frequency respectively. So we can see that the design covers all three ETSI, FCC, and ARIB frequency bands. This graph also can show the sensitivity of the antenna to detuning from the material. The deepness of the S_{11} graph changes by placing the tag on top of heavier dielectric material. The phase response graph shows that the transition from inductive side (positive phase) to capacitive side (negative phase) also happens exactly at 865 MHz and 950 MHz. The phase graph also gives valuable information about quality of matching. In other words, the phase graph shows how close is the design to the ideal matching condition.

A perfect matching is obtained by adjusting the centre point of the peak to peak on zero-crossing. However, when the tag is placed on top of different materials or even in close proximity to the other tags, the matching condition changes and some offsets from zero-phase line will happen. The offset value that can still give an acceptable matching condition is different, based on the different designs. According to my design experience, as it is shown in Fig 3.7, when the peak to peak value of phase graph is small (e.g. 0.5º), the offset value is also small (less than ± 0.2º). It means that if the effects of external factors (e.g. close coupling effect) make more than ± 0.2º shifts from zero line, it causes the mismatch condition. In case of larger peak to peak value for the phase (e.g. 2º), the offset value can be bigger and a good matching condition can still be achieved when offset is less than ± 0.8º. The peak values of the phase graph can be adjusted by changing some antenna design parameters that is discussed in chapter 5. Moreover, the limitations for having too big / small peak to peak value are also introduced in chapter 5.

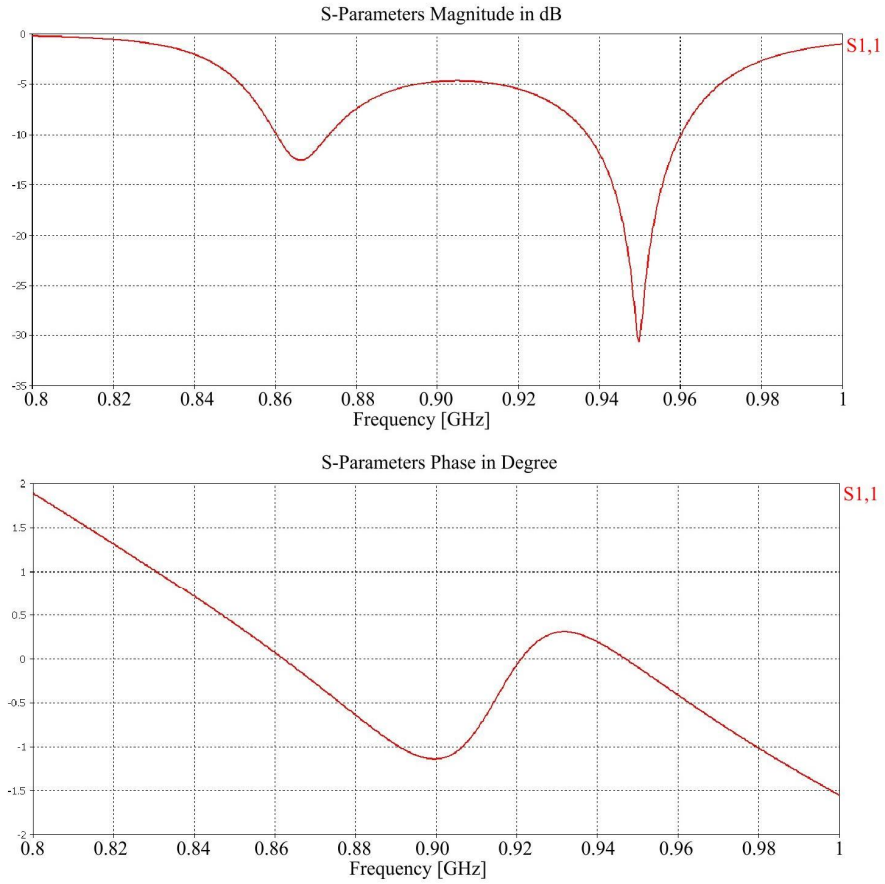

Fig 3.6. The S_{11} magnitude and phase diagram for Web tag.

Fig 3.8 presents the antenna radiation pattern. The maximum radiation (main lobe) is to the front and back side of the tag and, radiation minimum (side lobes) is to the both side direction of antenna. Based on the realized gain value, the expected read range is about 14 m (Fig 4.4).

To fulfil the design requirements, some part of antenna's skeleton should be adjusted many times and it needs redesign and repeated simulation work. There are always some tolerances between the simulated results and practical measurements since, the simulation is based on theoretical calculations and describes the ideal situation. In addition, there are some tolerances in production methods as well. To compensate the tolerances, the final design can be prepared in a matrix way with few different members of which finally one member meets the specification and become the final design. The etching process for Web antenna has been done by using the aluminium 9 µm as conductor and, PET 50 µm as substrate material. After face lamination and measuring the matrix members and selecting the final design, the samples are prepared for measurements.

First the frequencies of the samples were measured and one sample which has average frequency value was selected for application measurement. This way the effect of frequency variation can be eliminated. The application measurements made with Voyantic were performed in an anechoic chamber. To eliminate the effect of multipath

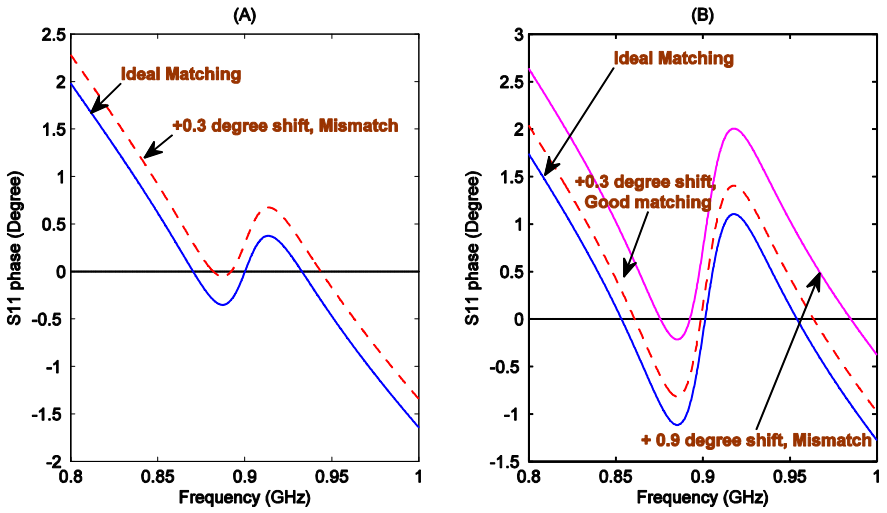

Fig 3.7. The offset from ideal matching condition in phase graph of S_{11}. (A): peak to peak value is about half degree, (B): peak to peak value is about two degree.

propagation on the measurements results, the calibration process was used before measurements. Measurement with Voyantic (Tagformance measurement system) is discussed in chapter 5 in more detail.

For average sample, the effect of material detuning has been measured by placing the tag on top of four different dielectric materials. The average sample has been placed vertically on top of these materials, in the distance of 50 cm from the Voyantic's reader antenna. Fig 3.9 shows the theoretical read range (Eq. 5.1) of measured average samples. The dielectric constant values of corrugate and free air are less than plastic and this is the reason why their radiator frequency is out of the band (more than 1GHz). About the PTFE material, which has highest dielectric constant value, the detuning effect of the material is shifted the radiator frequency to near 840 MHz, which is also out of range. The best performance has been achieved on top of the plastic material, as it was required. The performance of the Web tag in stack and under close coupling situation will be discussed in chapter 5.

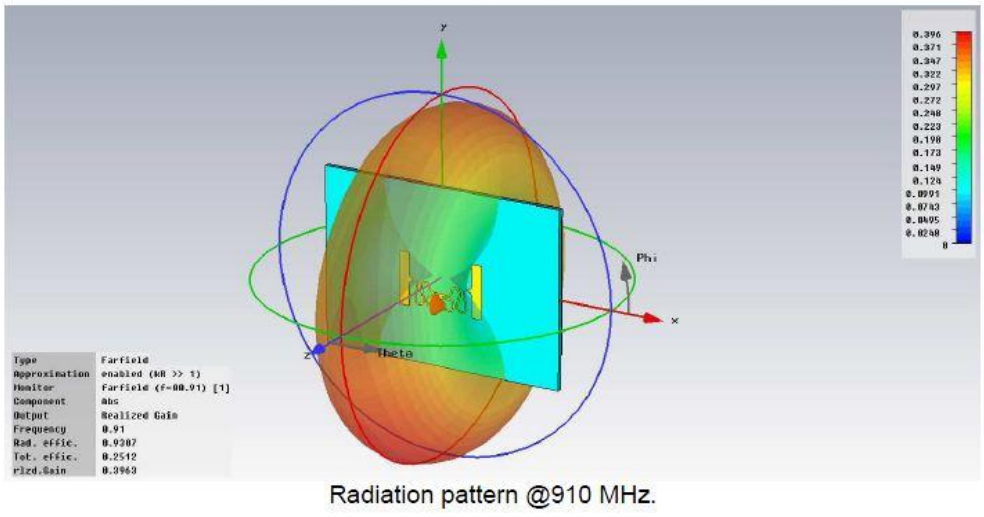

Fig 3.8. Radiation pattern of the Web antenna at 910 MHz.

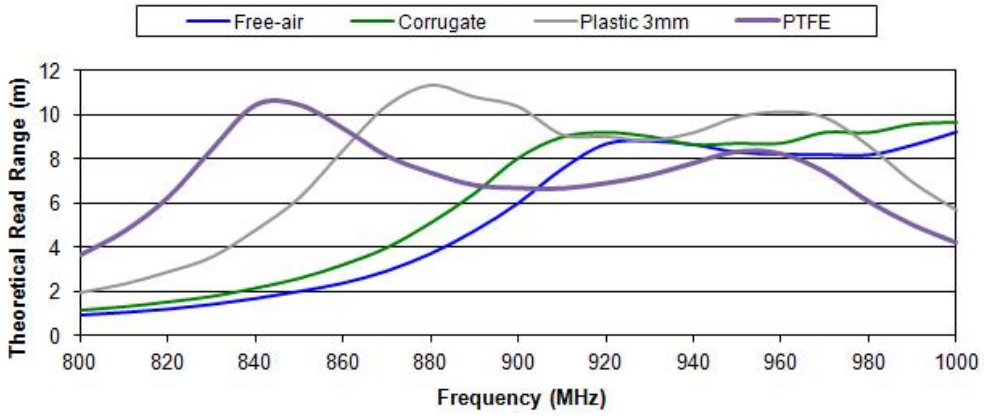

Fig 3.9. The read range of the Web tag on top of four different materials is measured by Voyantic set-up.

Chapter 4

4. Close Coupling Effect, Modelling and Analysis

In the previous chapter the main issues in design of a UHF passive RFID tag have been discussed. In most of the cases, the analysis of the performance of a tag is based on the assumption that the tag is communicating with reader alone [25], but there are applications for RFID tags in which tags are close together such as placement in stack. So it is important to design a tag that can meet the requirements as a stand-alone tag and also when it is placed in close proximity of other tags.

The performance drop is the biggest limitation of passive RFID tags in stacked applications. Designing a tag that can perform with the same performance in both applications is very challenging but there are some methods that can improve the performance of tags when the tags are placed close to each other.

Generally when an ordinary tag is placed in proximity of metal, electromagnetic coupling at the antenna of the tag will increase [26]. Now, when many tags whose antennas are metal become close to each other, they are affected by electromagnetic interference between each other and this causes a significant drop in read range and performance of each tag. The electromagnetic coupling effect between the tags is called as close coupling effect. The close coupling effect can happen for both HF and UHF tags when they are stacked in a near-field or far-field RFID systems. The close-coupling effect discussion for HF tags is not in the scope of this thesis. Also the coupling analysis of near-field UHF tags is not discussed in this thesis, but it is reported widely in the literature e.g. in [27], [28], [29] and [30]. However, when the passive UHF tags come close each other in a far-field RFID system, the electromagnetic modelling of behaviour of the system is more difficult to be done since more parameters are involved in communication between the reader and the tags. Although, the experimental evaluation

of the decrease of the read range, due to the interference between tags is already reported in [31], [32] and [33], the reasons that decrease the reader's reading rate are not sufficiently clear [35].

In the literature like in [25], [33], [35] and [36], the read range drop is explained from the standpoint of received power change in tags and reader. Since, the received power at the tag and the reader antenna is determined by impedance matching between the tag antenna and the IC, so from theoretical point of view, the analysis of tag antenna impedance in close proximity of other tags is significant. This chapter presents the theoretical model of close coupling effect from this point of view. The results are also verified with simulations.

4.1. Theoretical Analysis of Close Coupling Effect

In previous chapter we noticed that the best power transfer between the tag and the reader antenna can be achieved by having conjugate matching between tag antenna's impedance and IC's impedance. This matching condition changes when the tag is placed next to other tags. Deviation from the optimal impedance design causes the power loss in the system which will affect the performance of the whole system.

4.1.1. Change in matching condition due to closeness of tags

The electromagnetic coupling of antennas and mutual impedance has been studied widely in the literature, e.g., in [37] to [40]. The common conclusion is that when the tags are close to each other, the electromagnetic coupling of antennas will change the tag antenna's impedance because of the mutual impedance. In other words, the tag antenna impedance is deviated from the optimal impedance (conjugate matched) design by presence of the mutual impedance. Generally, when the distance between the tag antennas decreases and the tags get closer, the mutual impedance between antenna increases and it causes the deviation from the optimal design condition [34].

In order to study the mutual coupling between the multiple antennas, first consider the case of two antennas case. Then expand to the more antennas case. Fig 4.1 (a) shows two typical tag antennas that are connected to the loads (ICs) with the impedances Z_{IC1} and Z_{IC2}. Antenna 1 is activated with the voltage source V_1 (excitation voltage by reader) and antenna 2 is activated with the source V_2. If we also consider the antenna's impedances (Z_{A1} and Z_{A2}), the equivalent circuit model of the whole setup is shown in Fig 4.1 (b). As it is illustrated in Fig 4.1 (b), the electromagnetic field propagation of antenna 1 produces the extra voltage of V_{21} on antenna 2. In a same way, the electromagnetic radiation of antenna 2 introduces the extra voltage of V_{12} in antenna 1. Mutual impedance Z_{12} and Z_{21} explain the linear relationship between the voltage

sources V_{12} and V_{21} with the antenna's currents I_{A2} and I_{A1}, respectively. Applying the Kirchhoff's voltage law in both antennas circuit gives

$$I_{A1}(Z_{A1} + Z_{IC1}) = V_1 + Z_{12} I_{A2} \tag{4.1}$$

$$I_{A2}(Z_{A2} + Z_{IC2}) = V_2 + Z_{21} I_{A1}. \tag{4.2}$$

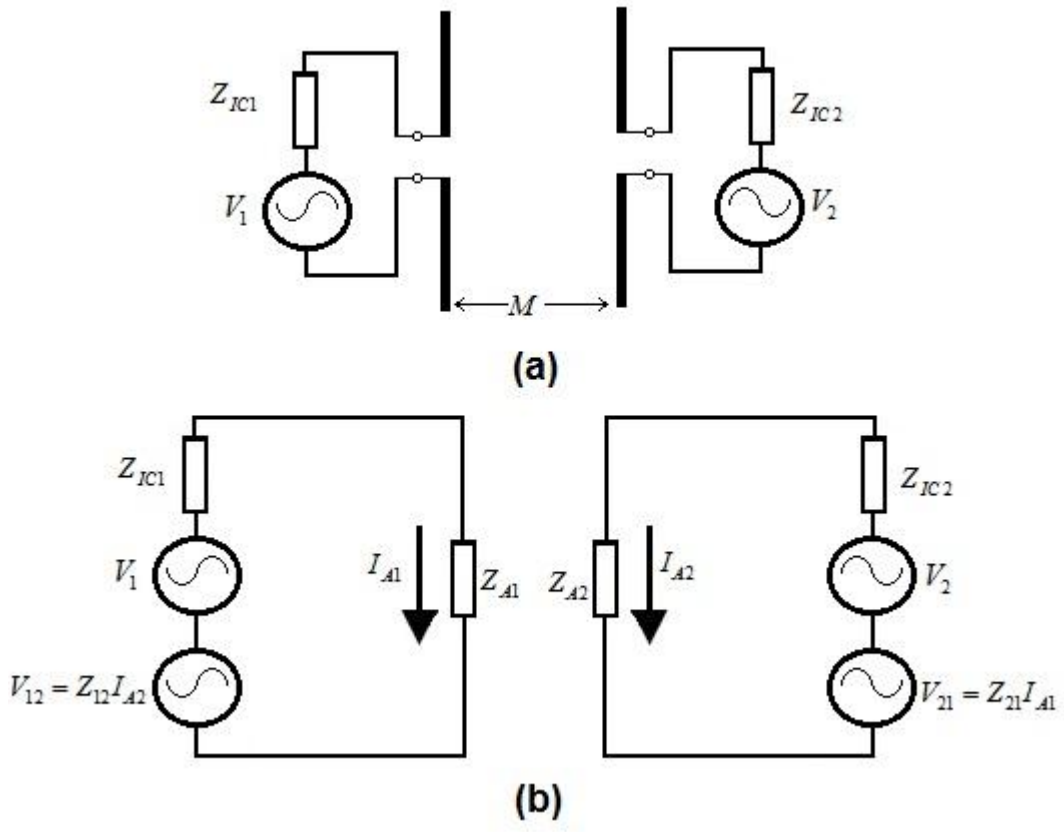

Fig 4.1. (a): Two dipole antennas placed in distance M from each other. (b): The equivalent circuits of antennas. Picture edited from [25].

The Eq. (4.1) and (4.2) can be written in matrix form as,

$$\begin{bmatrix} 1 & q_{12} \\ q_{21} & 1 \end{bmatrix} \begin{bmatrix} I_{A1} \\ I_{A2} \end{bmatrix} = \begin{bmatrix} V_1 / (Z_{A1} + Z_{IC1}) \\ V_2 / (Z_{A2} + Z_{IC2}) \end{bmatrix} \tag{4.3}$$

where q_{12} and q_{21} are normalized mutual impedances between antenna 1 and 2 and they are defined as [25]

$$q_{12} = \frac{-Z_{12}}{Z_{A1} + Z_{IC1}}, \tag{4.4}$$

$$q_{21} = \frac{-Z_{21}}{Z_{A2} + Z_{IC2}}. \tag{4.5}$$

In case of n antennas, the mutual impedance matrix is given as

$$\begin{bmatrix} 1 & q_{12} & \cdots & q_{1n} \\ q_{12} & 1 & \cdots & q_{2n} \\ \vdots & \vdots & \ddots & \vdots \\ q_{n1} & q_{n2} & \cdots & 1 \end{bmatrix} \begin{bmatrix} I_{A1} \\ I_{A2} \\ \vdots \\ I_{An} \end{bmatrix} = \begin{bmatrix} V_1 / (Z_{A1} + Z_{IC1}) \\ V_2 / (Z_{A2} + Z_{IC2}) \\ \vdots \\ V_n / (Z_{An} + Z_{ICn}) \end{bmatrix} \tag{4.6}$$

where, the normalized mutual impedance between the antenna i and j is defined as [25]

$$q_{ij} = -Z_{ij} / (Z_{Ai} + Z_{ICi}), \tag{4.7}$$

$$Z_{ij} = V_{ij} / I_{Aj} \ , \ (i, j \in N). \tag{4.8}$$

The simulation results in [35] and also equation (18) in [25] denote that, the mutual impedance is inversely proportional to the distance between the tags. It means when the distance between the tags increases infinitely, the mutual impedance value becomes zero. In addition, simulation results in [35] show that when the distance between the two tag antennas increases the real part (R) of the direct impedance (Z_{11}) increases while the imaginary part (X) decreases. In Eq. (4.1), if we suppose that the mutual impedance of Z_{12} is zero, the total impedance of the equivalent circuit is the summation of the antenna's impedance and the IC's impedance that are always complex conjugate matched (because the power loss becomes then the smallest). The effect of mutual impedance Z_{12} changes the matching condition of the antenna 1. The same is valid for antenna 2 by the presence of Z_{21} and also in the case of n antennas, when the matching of all antennas will change by presence of q_{ij}. Deviation from the optimal impedance design, by change of matching condition causes power loss in both forward and reverse links which is discussed in the next section.

4.1.2. Change in received power of reader and tag due to closeness of tags

As it is discussed above, the closeness of the tags changes the matching condition by changing the antenna's impedance, which causes the change of the received power both in reader antenna and the tags. This can be interpreted as change of read range [35], so it is necessary to explain the effect of impedance change on the received power.

Change of the received power by tag and reader antennas in close-coupling condition can be explained by modelling the power propagation in forward link (power flow from reader to tag) and reverse link (power reflection from tag to reader). According to the Friis equation and analysis in [35], the received power of tag in forward link can be expressed as [35]

$$P_e = (\frac{\lambda}{4\pi r})^2 P_R G_R G_T \left(\frac{4R_{IC} R_a}{(R_{IC} + R_a)^2 + (X_{IC} + X_a)^2} \right) \geq P_{e\_th} . \quad (4.9)$$

Similarly, for the reverse link, the received power of the reader is given as[35]

$$P_r = (\frac{\lambda}{4\pi r})^4 P_R G_R^2 G_T^2 \left(\frac{4R_a^2}{(R_{IC} + R_a)^2 + (X_{IC} + X_a)^2} \right) \geq P_{r\_th} \quad (4.10)$$

where, r is the distance between tag and reader antenna, P_R is transmitted power of the reader, G_R and G_T are the reader's and tag antenna's gain, respectively, R_{IC} and R_a are the IC's resistance and tag antenna's radiation resistance respectively and finally, X_{IC} and X_a are IC's and tag antenna's reactance, respectively. As it is shown in Eq. (4.9), (4.10), P_e needs to satisfy threshold electric power P_{e_th} and P_r should satisfy detection threshold power P_{r_th}. The effect of distance change on G_R and G_T is previously reported in [33], and for simplicity, change of the gains by changing the antenna's impedance is not included in the analysis here.

Fig 4.2 shows the reader and tag configuration when the second tag antenna is brought close to the first tag antenna. The second tag is placed in distance M from the first tag. Since in this analysis, the reader is placed far enough (more than 50 cm) from the tags, the effect of electromagnetic interferences of the reader can be neglected. In the previous section, we discussed how the presence of tag 2 affects the impedance of tag 1 (and vice versa). By presence of tag 2, the received power of tag 1 changes because of the change of impedances (Eq.(4.9)). Here, $P_e(M)$ is defined as received power of tag 1 when tag 2 is close to tag 1. Furthermore, $P_e(\infty)$ is defined as received power of tag 1 when tag 2 is placed at $M = \infty$ (the far enough from tag 1 that there is no close-coupling effect). From Eq. (4.9) we get [35]

$$\Delta P_e = \frac{P_e(M)}{P_e(\infty)} = \frac{\left| Z_{IC} + Z_A(\infty) \right|^2 R_a(M)}{\left| Z_{IC} + Z_A(M) \right|^2 R_a(\infty)} . \quad (4.11)$$

In the same way, change of impedance has also effect on the received power of reader. The received power of reader when distance between tags is M can be defined as $P_r(M)$ and when M goes to infinity, it is defined as $P_r(\infty)$. From Eq. (4.10) we get [35]

$$\Delta P_r = \frac{P_r(M)}{P_r(\infty)} = \frac{\left| Z_{IC} + Z_A(\infty) \right|^2 R_a^2(M)}{\left| Z_{IC} + Z_A(M) \right|^2 R_a^2(\infty)} . \quad (4.12)$$

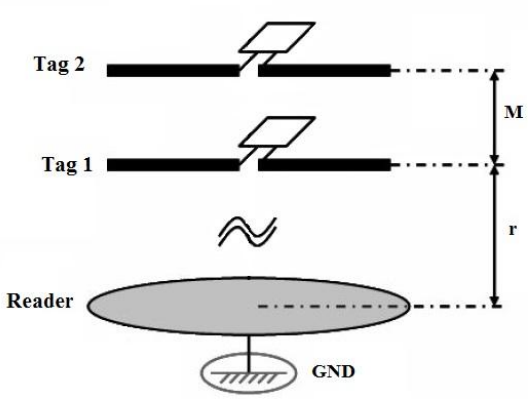

Fig 4.2. Tag 1 is placed in distance r from reader antenna and distance M from tag 2, where $r \gg M$. Picture edited from [35].

In both Eq.(4.11) and (4.12) the IC impedances ($Z_{IC} = R_{IC} - jX_{IC}$) are supposed to be constant and antenna impedance ($Z_A = R_a + jX_a$) varies with the distance M. The analytical results of Eq.(4.11), Eq. (4.12) show that both ΔP_e and ΔP_r are less than unity, and it means that in both cases, $P_{r,e}(\infty) > P_{r,e}(M)$. Therefore, this can prove that the received power of a typical tag in proximity of other tags decreases when compared to the case that tag is alone in front of the reader antenna. Furthermore, the received power of the reader antenna also drops when there is more than one tag in front of it compared to the case where we have a stand-alone tag in front of the reader antenna.

4.2. Simulation of Tags

The conclusions that we obtained from the theoretical analysis need to be verified by the simulator. The same design as in chapter 3 (Web design) is selected for the simulation. After importing the AutoCAD file into CST software (simulator), the antenna layout is placed on top of 50 μm substrate of PET material. The size of the PET layer is selected to be 150 mm by 100 mm. It is recommended to use the CST's RFID antenna template because the basic setting related to antenna simulation such as, dimension, frequency, temperature, time unit are set automatically. The boundary conditions are set equally and frequency range is set from 700 MHz to 1.2 GHz. Also the far-field setting is needed for calculation of the gain and eventually, the read range. The IC is modelled by impedance of $Z_{IC} = 30 - j169$ in simulation [23].

Fig 4.3 shows the simulation result for impedance of the Web antenna. From the real and imaginary graphs, the antenna impedance at resonant frequency (912 MHz) is about $Z_A = 42 + j150$. By substituting the antenna and IC's impedance in Eq. (4.13), the reflection coefficient is about $\Gamma = -24$ dB that means less that 1% reflected power and it shows very good matching. As it is mentioned before, the conjugate matching can only be achieved in one frequency point and it cannot stay valid for a broad-band design. However, this is the best matching situation to get a good performance from this antenna. The estimated read range by simulation for Web antenna is illustrated in Fig

4.4. Simulator calculates the read range according to the Eq. (4.14), where G_r (antenna's gain), p (the polarization loss factor) and s (S-parameters) are computed by simulation results, and P_{EIRP} (EIRP power transmitted by the reader), P_{th} (minimum power required to activate the chip) are defined to be 3.28 W and -18 dB, respectively [41][42]. The estimated read range in Fig 4.4 is close enough to the one in Fig 3.9 when the tag antenna is measured on top of the plastic material.

$$\Gamma = \frac{Z_{IC} - Z_A^*}{Z_{IC} + Z_A}. \tag{4.13}$$

$$R_d = \frac{\lambda}{4\pi}\sqrt{\frac{P_{EIRP}G_r}{P_{th}}\,p(1-|s|^2)}\,. \tag{4.14}$$

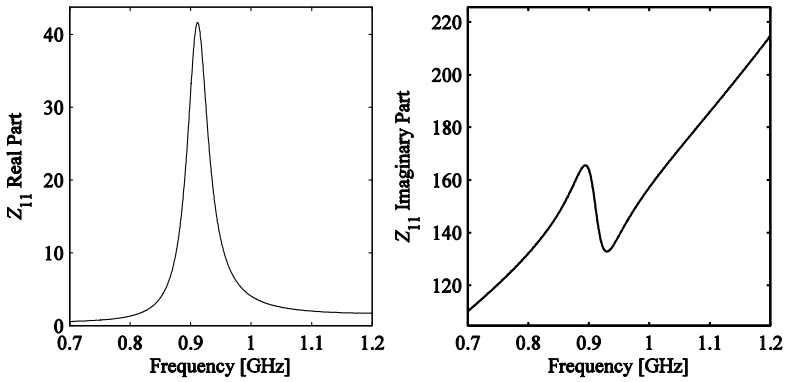

Fig 4.3. The Web antenna's impedance. $Z_A = 42 + j150$ at 912 MHz.

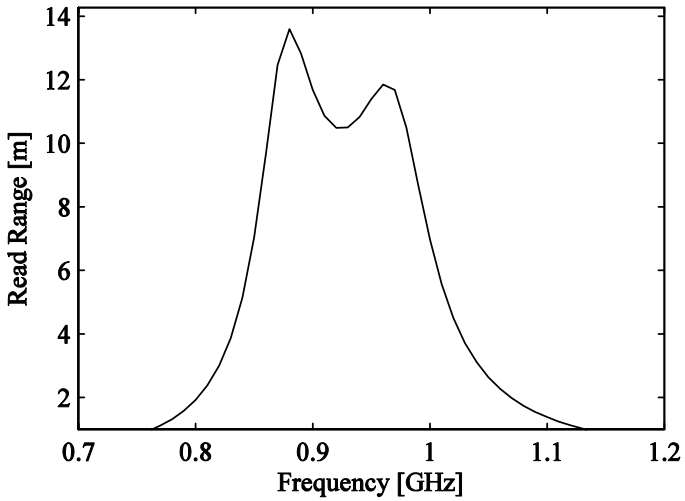

Fig 4.4. Estimation of the read range by simulator for single Web tag.

In the next step, the effect of proximity of other tag on the antenna performance is studied. Fig 4.5 shows the other Web antenna which is placed in distance of 25 mm from the first web antenna. The chosen distance is same as the distance between the tags in stack in actual measurement, according to UofA test procedure. As it is mentioned in Section 4.1.1, the tag antenna's impedance changes when it is placed in close proximity of the other tag antenna. The change of antenna's impedance is illustrated in Fig 4.6 and

it is not anymore matched with IC's impedance. As it is denoted in theoretical analysis, the real part of the impedance increases while the imaginary part decreases. This deviation from the matching condition, changes the tags performance as it is shown in Fig 4.7. There is about 1 m performance drop estimated by the simulator. The second Web tag's impedance (Z_{22}) looks similar to Z_{11} and also, the mutual impedance graphs (Z_{12} and Z_{21}) look exactly the same for both tags. This shows that the effect of two antennas on each other is the same. However, in the case of having more antennas it is not similar.

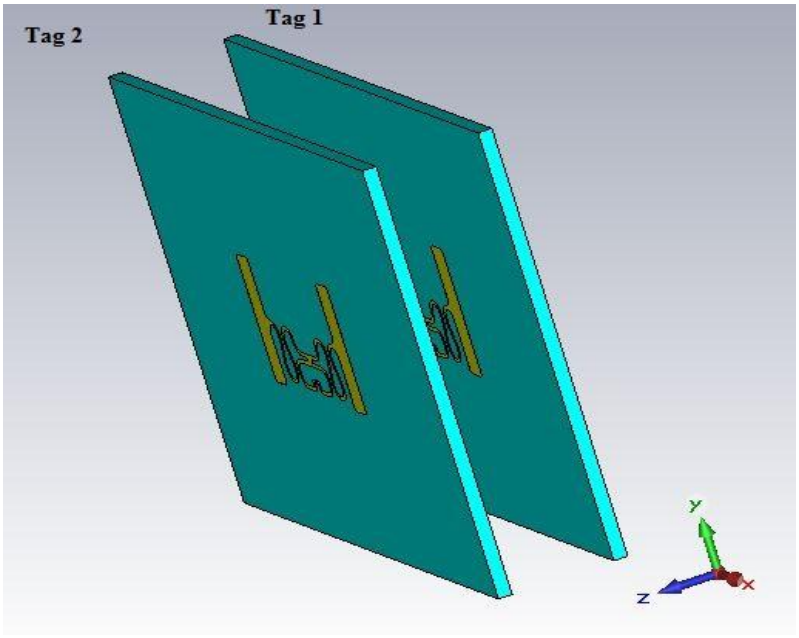

Fig 4.5. Two Web tag in the distance of 25 mm from each other.

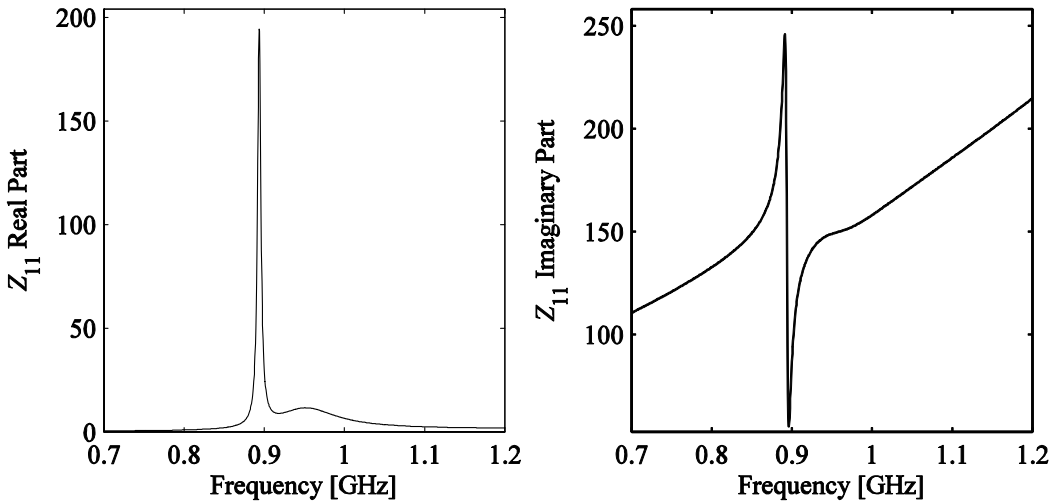

Fig 4.6. The impedance of tag 1, $Z_A = 183 + j105$ at 895 MHz, in the close proximity with tag 2.

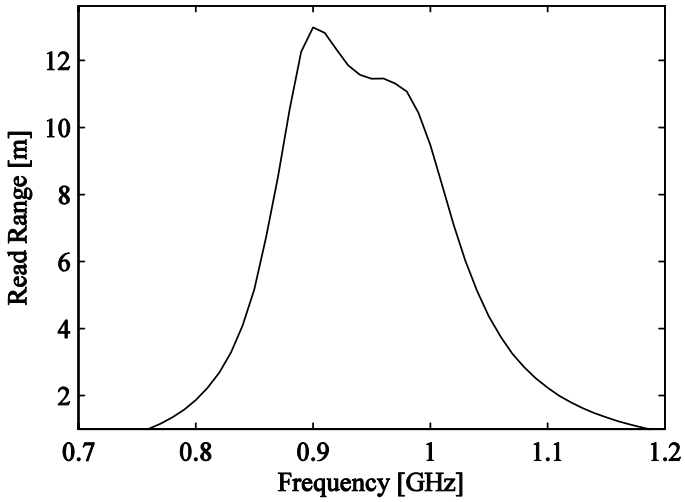

Fig 4.7. Estimation of the read range by simulator for the Web tag in proximity of other Web tag.

The next case is done by placing 7 Web tag close together (Fig 4.8). The simulation results that show the impedances for 7 tags are left out because of complex appearance. However, the results denoted that the top most (tag 7) and bottom most (tag 1) tags have closest impedance behaviour to Fig 4.3. After these two, impedances of tag 2 and tag 6 have less deviation from the matched impedance condition compared to the tag 3 and tag 5. And the middle most (tag 4) tag's impedance has most deviation from Fig 4.3. Therefore, it is predictable that the best antenna's performance belongs to the most top and the most bottom tags. It was not possible to plot the read range of 7 antennas separately by this simulator, but instead the average read range result is shown in Fig 4.9.

As consequence, the simulation results show that increasing the number of the tags causes more change in each single tag's impedance and decreases the performance of the tags more. In the next chapter we will measure the simulated case practically and will compare the simulation results with the actual measurements.

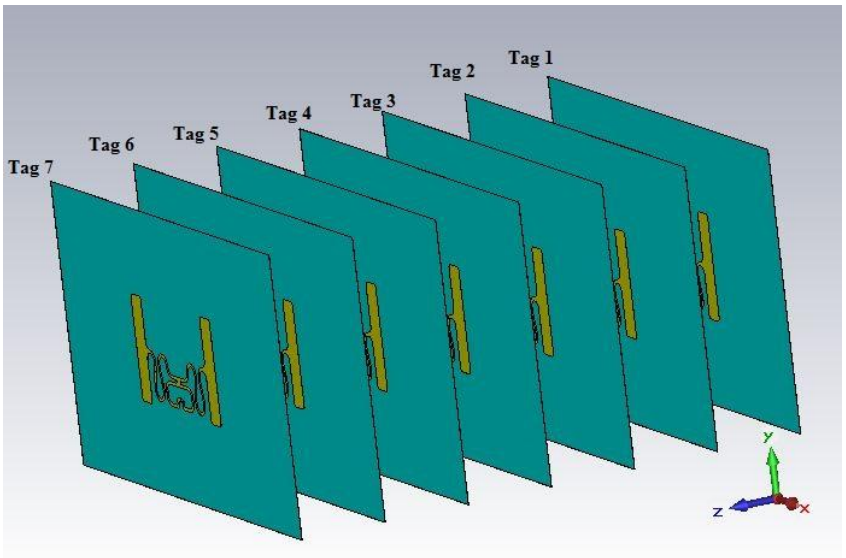

Fig 4.8. 7 Web antennas with distance 25 mm from each other.

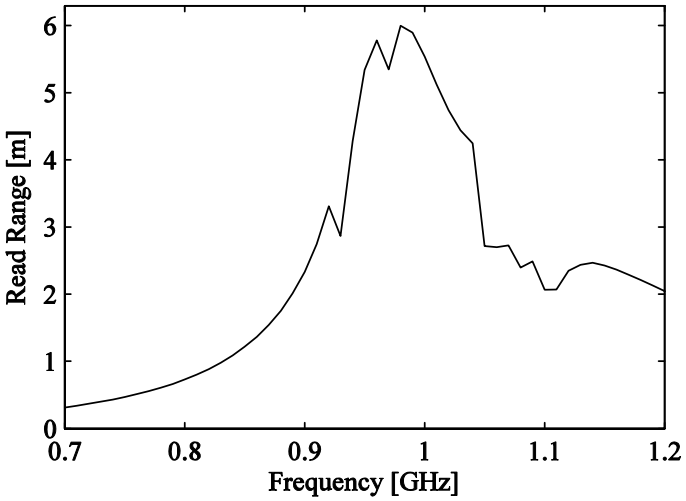

Fig 4.9. Average read range of 7 Web tags is estimated by simulator.

Chapter 5

5. Measurement, Development and Verification

In chapter 3 the necessary issues about design of the tag antenna have been summarised. The close coupling effect, as a limitation in performance of the tag antennas in some applications, has been discussed in chapter 4 from theoretical point of view. In addition, the previous researches about this topic were reviewed in the chapter 4. Here, a practical approach in design of the UHF tag antenna, for improvement of close coupling effect, is presented. The purpose of the study is to find the dominant parameters in design of the tag that have influence to the close coupling effect.

The Smartrac product (Web antenna) which is designed for stacked application is selected for more survey. First, the performance of the Web tag antenna in stacked application will be measured. Then, for this specific antenna, by redesigning of matching point, we can see the effect of the design's parameters on performance of the tag in close coupling environment.

The measurements are conducted based on the standard type of the testing methodology. It is according to the University of Arkansas Radio Compliance (ARC) center tests. Since, The University of Arkansas (UofA) RFID research center is the first academic laboratory accredited by EPCglobal [43].

5.1. Measurement Set up

Tagformance Measurement System

All the application measurements are conducted in an anechoic chamber by using Tagformance measurement system, which is known as Voyantic set up. The Tagformance measurement system includes a Tagformance lite reader, a reader antenna and the Tagformanc software running on the PC. This measurement set up is a network analyzer optimized for far-field measurements of RFID tags. The reader antenna should be placed inside the shielded and anechoic chamber to be isolated from the

environment's interferences. Typically for measurement of the performance of a single tag, distance of about 30 to 50 cm is good choice in order to minimize the effect of reflections and possible interference. Tagformance lite is a bistatic reader unit consisting of a radio frequency generator and an RF receiver with the sensitivity of - 80 dBm. The reader offers measurement frequency range of 800-1000 MHz. The Tagformance software supports the standard protocol of EPC Class 1 Gen 2 (ISO18000-6C), and the forward modulation is DSB-ASK with PIE encoding. For measurement of the single tag the command ISO 18000-6C Query is selected and for the stacked measurement of the tags, the command of ISO 18000-6C Select+Query can be used to address the tag selected in the tag list of the Population management panel. Before doing the actual measurement, system must be calibrated. A reference tag antenna is provided by Voyantic for calibration. The wideband calibration tag can be used for calibration of 700 MHz to 1200 MHz frequency range. After calibrating the set up, different type of the measurement such as threshold, orientation sensitivity and backscatter measurement can be done with Tagformance system. The theoretical read range estimation by the Tagformance is done based on the threshold power measurement. The threshold power is the minimum transmitted power by Tagformance that can make the tag active. After power measurement, the theoretical read range is calculated by Eq.(5.1), where $P_{\max,EIRP}$ is the maximum allowed transmit power defined as EIRP power and its default value used is 3.28 W. [41]

$$R_{\max} = \frac{c}{4\pi f}\sqrt{\frac{P_{\max,EIRP}}{P_{tag}}} \tag{5.1}$$

UofA Test Procedure

The University of Arkansas (UofA) RFID research center is one of the first EPC/RFID research laboratories worldwide to receive the EPCglobal performance test center accreditation. The purpose of the Arkansas Radio Compliance (ARC) center is to ensure that the retail suppliers are able to deliver RFID tagged product to retailers that meet or exceed the criteria to provide benefit to both the retailer and the retail supplier in a consistent and cost effective manner. The ARC testing methodology offers different type of the test for specific levels of inlay performance. The UofA research center currently co-chairs the Accredited Test Center Council, a group comprised of all of the accredited test centers, and has taken a leadership role in developing standardized testing methods among accredited labs. [43]

Since the Smartrac UHF products are qualified for retail and apparel solutions by the RFID Research Center of University of Arkansas, the measurement procedure of the tags which are explained in this chapter, follow the UofA protocol. In the other words, the measurement set up, adjusting the measurement power, frequency, and distance, the

used material and steps of measurement are according to ARC testing methodology version 1.37 published in December 7, 2010 [44].

5.2. Measurement of Web Tag Antenna

In the previous chapter the simulation of the Web antenna was discussed. The simulated read distance for one tag case was close enough to the measured value in Fig 3.9. Here we are going to compare the performance of one tag with multi tags in the stack.

Frequency measurement

To get more precise results from stacked measurement, it is better to select uniform samples for the measurement. In order to cancel the effect of the frequency variation between the samples and have uniform samples, the resonant frequency of the 30 samples is measured. Then 7 samples from 30 samples are selected for measurement in stack. According to the UofA instruction, 10 samples should be used for stacked measurement, but here 7 tags have been selected for simplicity and also to speed up whole measurement process.

The resonant frequency of the samples is measured by unloaded resonant frequency

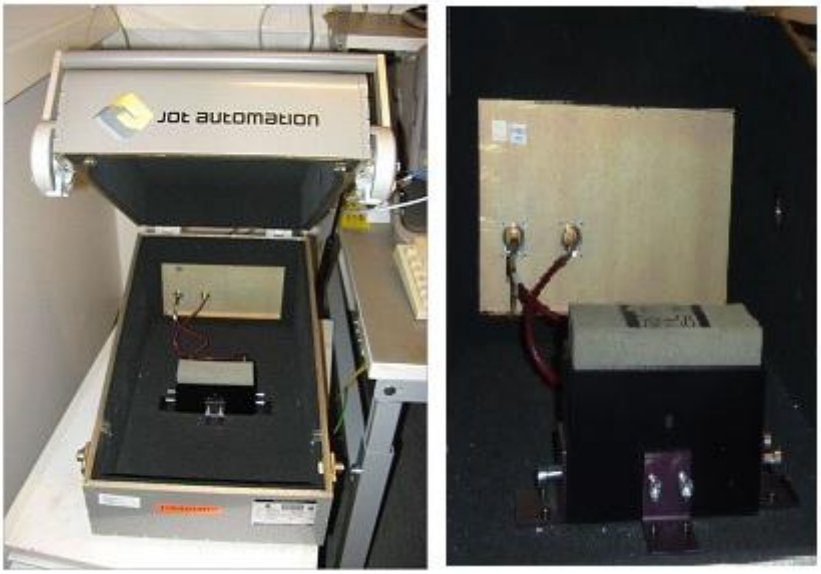

Fig 5.1. Unloaded resonant frequency of the Web tag is measured inside JOT chamber.

measurement set up. As it is illustrated in Fig 5.1, JOT anechoic measurement chamber is used to improve the measurement accuracy, since the chamber is free of the other radio signals and provides an interference free environment for measurement. The frequency measurement is done using the sniffer antenna which is placed inside the chamber. The chamber is connected to a spectrum analyzer for measuring the frequency. Before starting the product measurement, set up is calibrated with the calibration samples to be sure that the set-up is working right. Then the Web tag sample is placed into the chamber on the top of the sniffer, and by adjusting the frequency span from spectrum analyzer, the resonant frequency peak value is measured. After

measuring 30 Web samples, the average frequency was about 925 MHz. One sample that has closest frequency to the average value is selected as average sample (S6). Also, 6 more samples (S7, S8, S9, S11, S13 and S15) which have closer frequency to the average samples have been selected for the stacked measurement.

Application Measurement

As it is explained, the measurement is done according to the part of UofA application measurement steps. The application measurement is also conducted in a shielded anechoic chamber by using Tagformance set up. According to the UofA test procedure, in the first step, the single inlay is measured in the free air and on top of the denim material. The reason for using the denim material is to evaluate the product performance in an actual measurement case which directly benefits the customer.

Free air measurement of one Web sample is shown in Fig 5.2 (a). The average sample (S6) is placed horizontally on top of the styrofoam, in front of the linear polarized reader antenna in distance of 50 cm from the antenna. Same measurement in same distance is also done for the average sample, on top of the denim material. The attachment of the sample to the denim is done according to the Fig 5.2 (b). The average sample without backing paper is attached to the product's label that is placed on top of the denim with the thickness of the 25 mm (the attachment of the sample is similar to the labelling in the stores). The threshold measurement is conducted and the read distance of the tag in both measurements is shown in Fig 5.3. It should be noticed that the difference between the read ranges in the Fig 3.9 and also the simulation result of the Fig 4.4, with the Fig 5.3 is because of the direction of the tag in front of the reader antenna. In the Fig 3.9, the tag is placed vertically in front of the reader antenna, while here it is placed horizontally. From the Fig 5.3, the measurement result of the single inlay shows the maximum read distance of 8.5 m for both free air and denim cases.

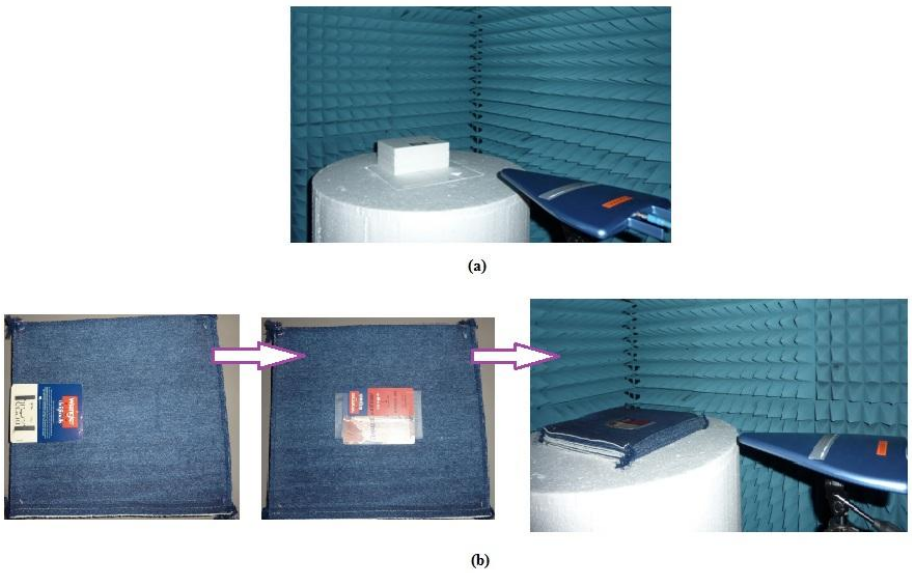

Fig 5.2. Measurement of the single Web tag (a): in the free air, (b): on top of denim material.

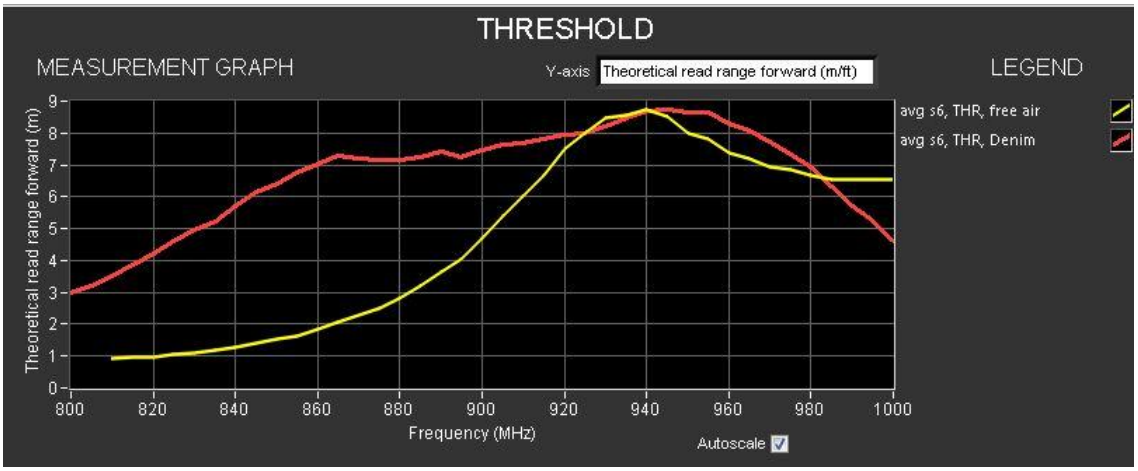

Fig 5.3. The read range of the single tag in free air and the denim material.

In the second step, multi tag measurement in stack is done. Before that, the population list for the 7 tags, which are already selected according the frequency measurement, need to be created. From the population list, we can select the tag one by one to communicate with the reader. By this way, interaction between the tags and reader follows the anti-collision protocol and it means that, although all the tags are placed in the field generated by the reader, but only one tag will response to the reader's interrogation [30], [41]. The order of the tags in the tag list is in the same order of the placement of the tag in front of the reader. It means that, the top most tag in the list is also the top most one in the stack front of the antenna. Fig 5.4 shows 7 Web tags which are in the stacked in free air.

To be closer to the simulated conditions, the overlap between the tags is tried to be maximized. However, in practical measurement it is hard to have 100% overlap between the tags and only iteration the measurement can help to become closer to the 100%. The thickness of the spacers between the tags is 25 mm. The reader is in the distance of 50 cm from the middle most tag. The theoretical read ranges of the tags are illustrated in Fig 5.5. The results are comparable to the estimated result by the simulator (Fig 4.9). The comparison between the free air results of the Fig 5.3 and the Fig 5.5, shows that the performance is decreased about 3 m, by placing the tags close together. Furthermore, as it was predicted from the simulation, the top most (S6) and bottom most (S15) tags show the best performance compared to other tags, since the less impedance change happens for these two tags. The middle most tag (S9) has the worst performance. The behaviour of the other tags also follows the simulation results except S13 that should be closer to the red line (S7).

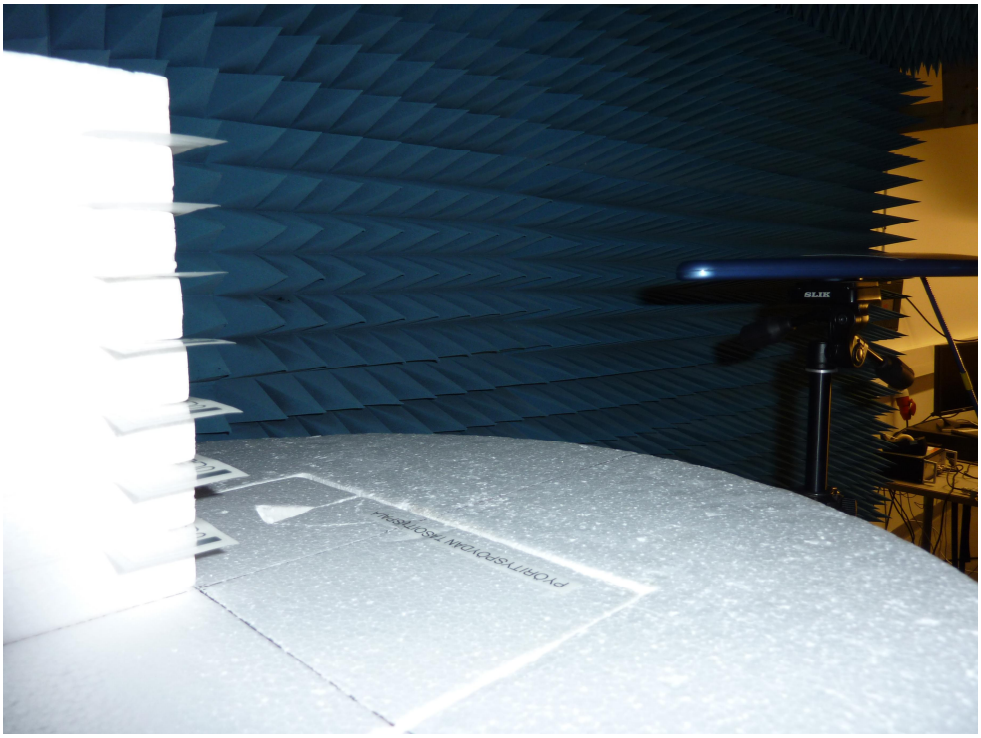

Fig 5.4. 7 Web tags in free air stacked, in front of the reader antenna.

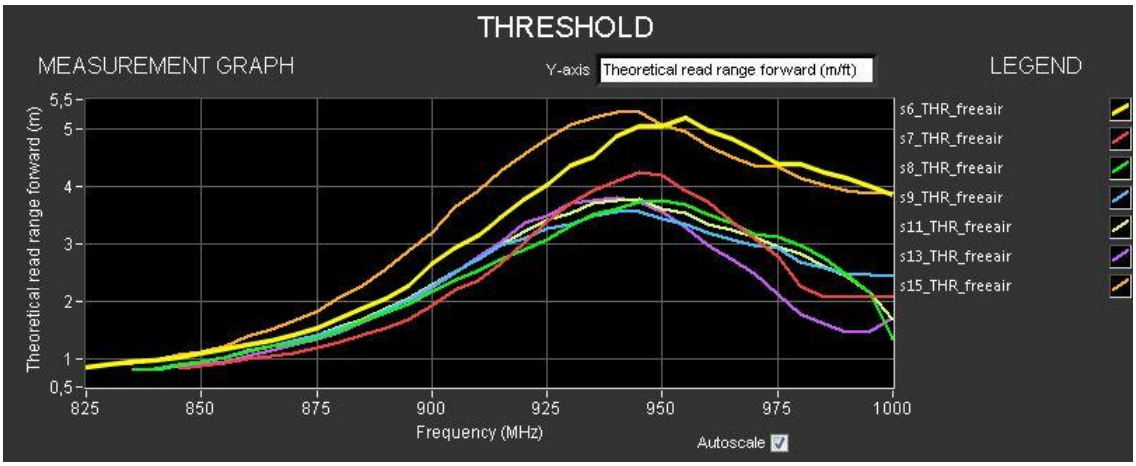

Fig 5.5. The read distance of 7 tags in stack in the free air.

In the next and last step, 7 tags are placed in the stack, on top of the denim in front of the reader antenna (Fig 5.6). Each single tag is attached to the denim whose thickness is 25 mm and then 7 denims are placed on top of each other. The attachment of the tags to the denim is done in the similar way as the Fig 5.2 (b). The measurement process is same as the free air measurement. The measurement results in Fig 5.7 show performance drop of about 3 m in comparison to the single inlay on top of denim. However the top most tag has the smallest drop in performance, because of lesser influence of the other tags.

As an overall conclusion in this part, the performance drop of the stacked tags for both free air and denim measurement is almost the same. We know that free air is a low dielectric constant environment but denim can be considered as a “heavy” environment

(ε is about 2). The measurement results denote that the performance of the Web tag in stack, in this wide range of the different material, does not vary that much and it is stable. This can be considered as a positive point in the design of a product for close coupling environment, since the performance does not change too much by changing the application material.

The Web tag performance in close coupling has been studied in this section. Even though the results eventually meet the UofA performance criteria, in the next section, we are going to improve the performance of this product in close coupling situation even further.

Fig 5.6. 7 Web tags are measured on top of the denims.

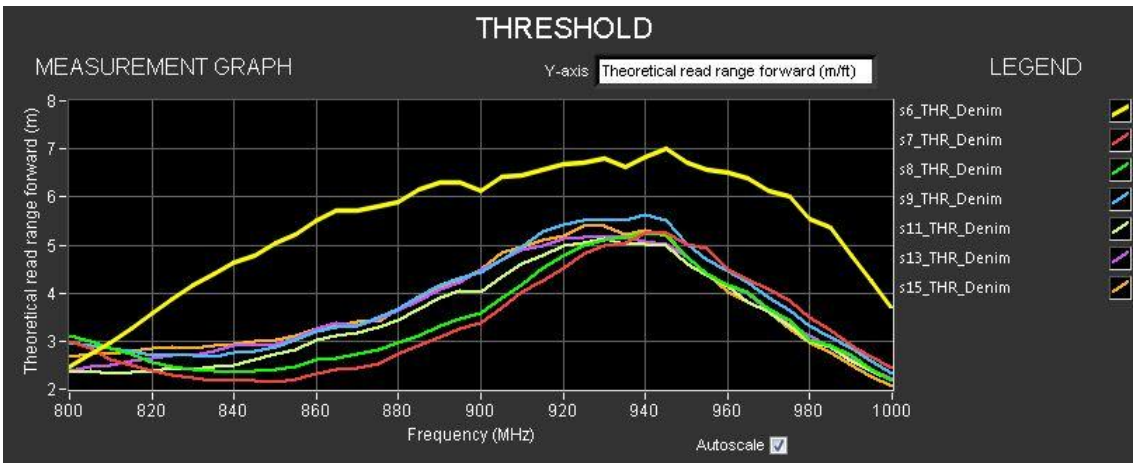

Fig 5.7. The read distance of the tags in the stack on top of denim.

5.3. Improvement of Web Design for Better Close Coupling Performance

Some parameters that have influence to the behaviour of the tags in close-coupled situation have been explained in detail in chapter 4. Based on that information, and also the effective parameters for the design of a good performance UHF tag antenna (reviewed in the chapter 3), some practical methods for optimizing the performance of the tag in close coupling environment is introduced. Optimizing the design for minimizing the close coupling impact, should not change too much the performance of the single tag. However, there will be a trade-off between the performances of a tag as an individual tag and in close proximity with other tags.

As it is explained in the previous chapter, most of the close coupling effect happens due to change in the matching conditions. From theoretical point of view, many different parameters have influence to the matching condition, and it is impossible to survey all of them at the same time and involve them in the practical design. However, from the actual design point of view, the design properties of the matching point can be considered as primary aspect that affect the matching conditions.

From the chapter 3 we noticed that, in the design of a tag antenna, the reflection coefficient (S_{11}) is a graph that can describe the matching condition properly. The magnitude graph of S_{11} describes the ratio of the reflected wave to the amplitude of the incident wave [42], and it is also an indicator for sensitivity of tag to the material detuning effect. In addition, the phase graph of S_{11} shows the quality of the matching. Therefore, the design properties of the matching point will be studied here by considering the S_{11} graph. Every change in the matching condition, cab be observed in the phase graph of the S_{11}.

Here, the existing design of the Web tag is considered as a reference for performance enhancement in close coupling. By changing the matching condition of the Web, we are going to find where is the optimum tuning to achieve a better close coupling performance. The matching condition will change by changing the design of the matching point of the Web and finally, the result will be compared with reference Web antenna. This should be emphasized that, the design of the radiator element of the Web tag does not change, since by changing all the design parameters at the same time, no beneficial result can be obtained. Moreover, the matching point redesign found to be primary aspect.

Simulation

As it is illustrated in Fig 3.6, the peak to peak of the phase graph of the Web antenna is about 1.5 degree. By redesign of the matching point of the Web, we are going to adjust the peak to peak of the phase graph to the 0.5 degree and 2 degree. This will show that,

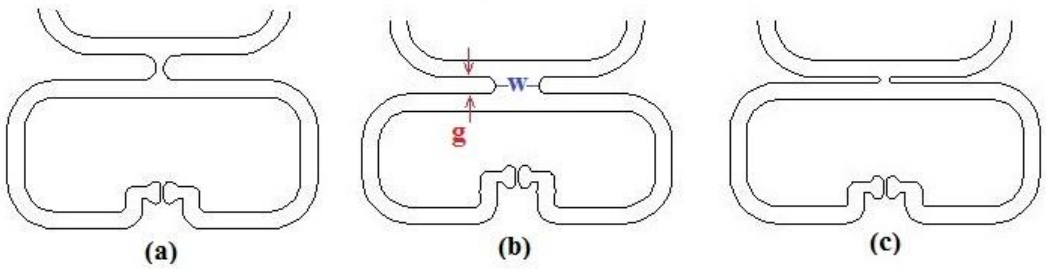

Fig 5.8. The redesign of the matching point and loop area of the original Web. (a): Web_MHD, (b): Web_ original, (c): Web_PHD

how a small change in matching point design, that cause $\pm 0.5°$ shift in phase graph (of the original Web), affect the tag performance.

Couple of iteration circles of design and redesign is needed between AutoCad and CST simulator to find the correct size/shape of the matching point that causes the $\pm 0.5°$ shift in the phase graph. The Fig 5.8 shows the difference between the matching point design of the original Web antenna and two new versions design for achievement 0.5 and 2 degree phase. To decrease the phase of the original Web from 1.5 degree to 0.5 degree, the width (w) of the matching point of the Web antenna is decreased. Because of the production limitation, the width cannot go below 0.3 mm. To further to decrease the phase, the gap (g) between the loop and the radiator has been change. The 0.5 degree phase is obtained by decreasing the width of the original Web from $w = 2.35\,\text{mm}$ to $w = 0.39\,\text{mm}$, and increasing the gap from $g = 0.93\,\text{mm}$ to $g = 1.39\,\text{mm}$. Fig 5.8 (a) shows the final matching point design for p-p $0.5°$ phase which is named as Web_MHD (Web_Minus Half Degree). In a similar way, to increase the phase from 1.5 degree to 2 degree, the width got narrower, from $w = 2.35\,\text{mm}$ to $w = 0.48\,\text{mm}$ and the gap also decreased from $g = 0.93\,\text{mm}$ to $g = 0.3\,\text{mm}$. As it is illustrated in Fig 5.8 (c), this new layout is named as Web_PHD (Web_Plus Half Degree).

The new layouts of the matching point cause small shift in the resonant frequency. The frequency shift can be ignored at this part, because it can be fixed later by changing the other terms. So the results are still comparable with the original Web, as long as the center of the peak to peak of the phase is adjusted on zero-crossing line. Adjusting the center of the peak to peak is required since, it causes the best matching condition to obtain the maximum performance and have a balanced read range in whole bandwidth.

The center point of the peak to peak can be adjusted on zero phase line, by changing the inner area of the loop. In fact, varying the inner area of the loop will change the inductance of the antenna (in the loop area). The inductance change can push/pull the phase graph toward/from zero line. Fig 5.9 shows the final simulation results of the new antenna layouts. From the figures we can see that the peak to peak value for Web_MHD

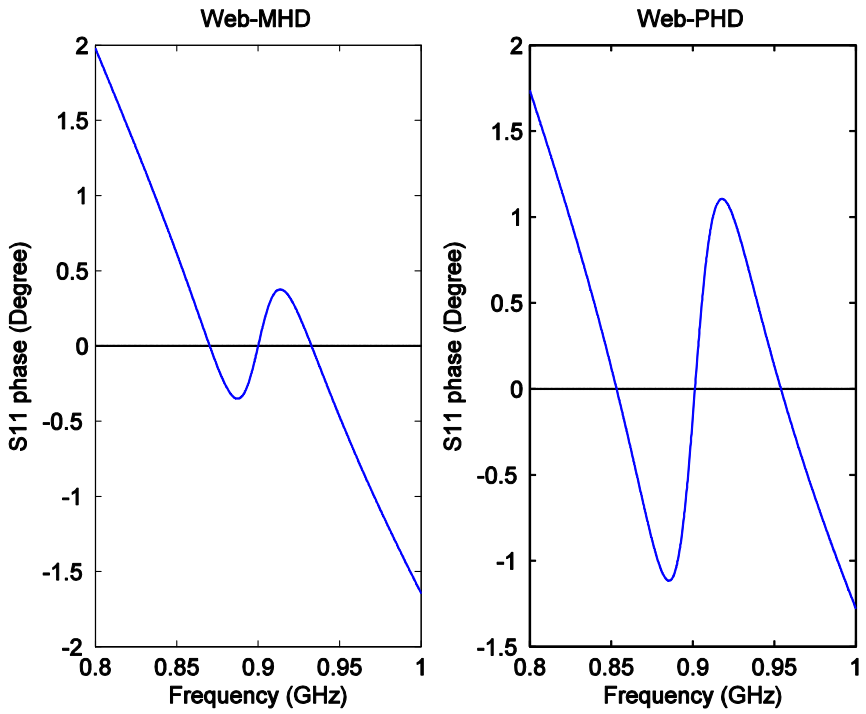

Fig 5.9. The S_{11} phase graph for the Web_MHD and Web_PHD.

is about $0.7°$ and for Web_PHD is about $2.2°$, which are close enough to the target. In addition, for both cases the center of the peak to peak is adjusted on zero phase line.

Measurement

After preparing the new versions of the Web, the samples are measured. The frequency measurement was done by preparing 15 samples of each design. For Web_MHD, the sample 8 is selected as average sample and S2, S4, S6, S7, S9 and S14 from 15 samples are selected for stacked measurement. Similarly, for Web_PHD, the sample 7 is selected as average sample and S1, S2, S3, S6, S8 and S9 from 15 samples are selected.

As it is also mentioned in chapter 3, the best performance of the Web can be achieved on top of the plastic material. So, the first step is the measurement of the average samples in the free air and on top of the plastic material. The average sample of the Web_MHD and Web_PHD are measured in front of the reader antenna in vertical position. The distance of the tag from the reader antenna is 50 cm. Fig 5.10, shows the measurement results of the average samples in free air and on top of plastic for original Web, Web_MHD and Web_PHD. The Fig 5.10 shows the same maximum performance for the Web_original and the Web_PHD in the free air and both of them have better

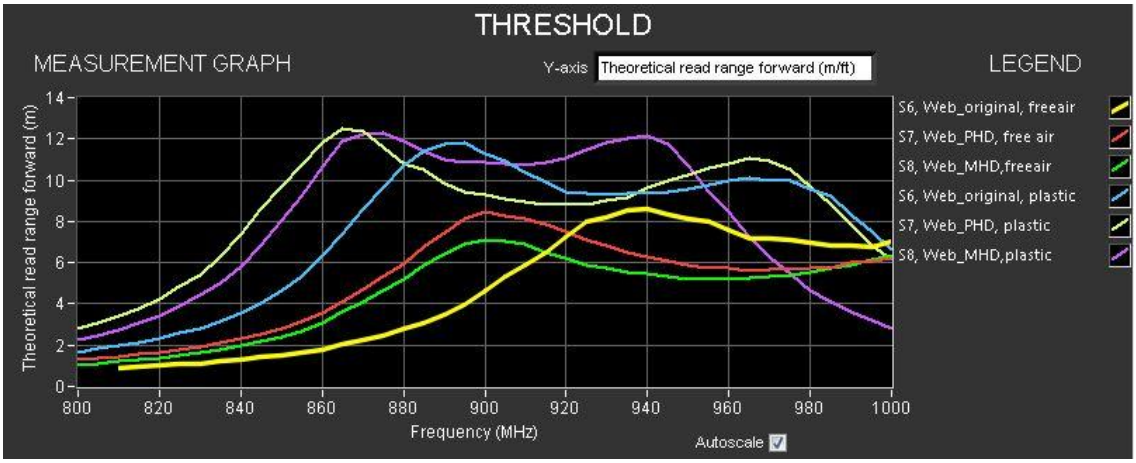

Fig 5.10. Read distance results of the average samples measurement for the Web_original, the Web_MHD and the Web:PHD. The Frequency shift between the designs can be neglected since it is secondary issue here and the maximum performance is considered as primary.

performance than Web_MHD. However, by placing the samples on top of plastic and tuning the right frequency band, the Web_MHD and the Web_PHD, have better read distance compared to the original Web. Furthermore, the Web_PHD has wider bandwidth compare to the others and also keeps the good performance in both dielectric constant situation.

The second step is the measurement of the 7 samples in the free air stack. The measurement procedure is exactly the same as the Fig 5.4. The measurement result for Web_MHD and Web_PHD are illustrated in Fig 5.11, Fig 5.12 respectively. Comparison between Fig 5.11 and Fig 5.12 with Fig 5.5 (original Web in the free air) denote that the higher read range belongs to the Web_PHD tags and the lower performance is for Web_MHD tags. The Web_original performance is something between two other designs, however it has the minimum variation between samples in peak performance value, compared to the Web_MHD and Web_PHD.

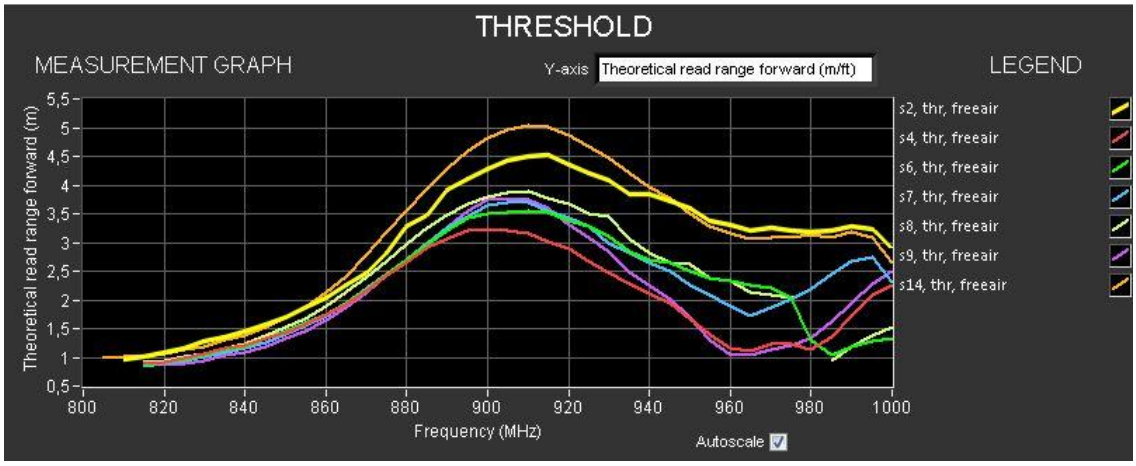

Fig 5.11. The read distance of the Web_MHD tags in the stacked in the free air.

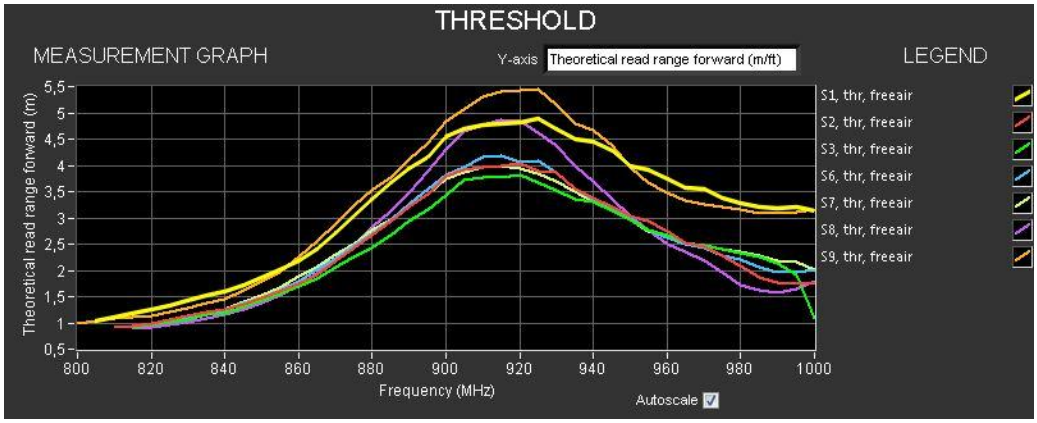

Fig 5.12. The read distance of the Web_PHD tags in the stacked in the free air.

The third and last measurement is conducted by placing the Web_MHD and Web_PHD samples on top of the denim (same as Fig 5.6). The measurement results are shown in Fig 5.13and Fig 5.14. Comparing these results with Fig 5.7 (original Web on the denim) shows the same conclusion as the free air case. Web_original shows the less variation between the samples compare to the new designs. And its overall performance is better than Web_MHD and worse than Web_PHD. However, all the designs on top of the denim have higher read range compared to the free air. The reason for higher performance is due to the higher effective permittivity, and the frequency tuning effect of the materials which can adjust the conjugate matching in right frequency.

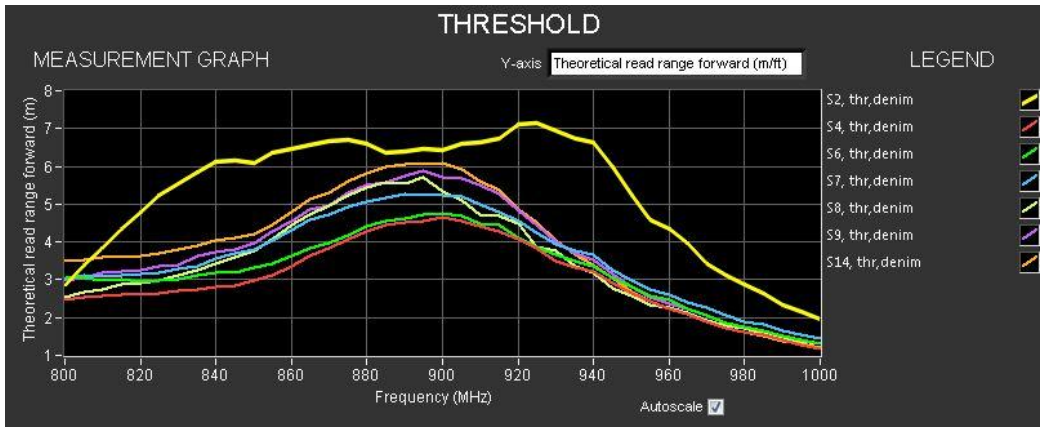

Fig 5.13. The read distance of the Web_MHD tags in the stacked on top of the denim.

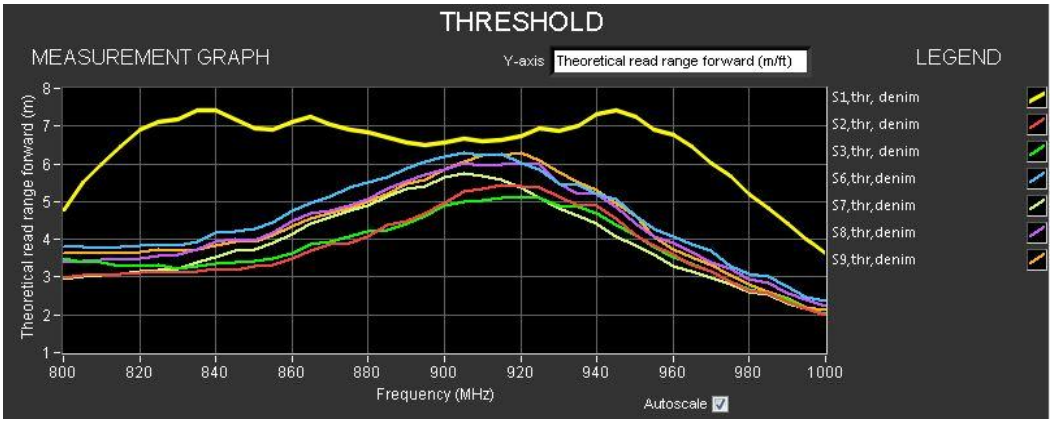

Fig 5.14. The read distance of the Web_PHD tags in the stacked on top of the denim.

5.4. Comparison and Discussion

By analyzing the measurement result, it is possible to obtain an optimal model for design of the matching point to decrease the close coupling effect.

Comparing the shape of the matching point for 3 different designs shows that the narrower the gap (g) is, the more peak to peak value for the phase can be achieved which gives the better close coupling performance. Furthermore, the higher phase peak to peak value enables wider bandwidth. However, from Fig 5.10 we can see that the narrower widthness for the matching point, the better the read distance but it also has negative effect to the variation between samples in the stacked measurement. The other affecting factor in matching point properties is the inner loop area. The smallest inner loop area (smallest loop inductance) belongs to the Web_original and the biggest area is for Web_MHD.

The result of the multi tag measurement denotes that, higher phase peak to peak value (Web_PHD) gives better performance in close coupling. The reason is that a good matching condition is available as long as the peak values of the phase graph are close enough to the zero-cross line. When the peaks go too far (in this case more than $\pm 0.8°$) from the zero line, the conjugate matching is not optimal any more. Now if there is a small peak to peak value (Web_MHD), the detuning effect of the materials and also the effect of other tags, can push the peaks far away from the zero line, faster than the case that there is higher peak to peak value. In the other words, the matching conditions for higher peak to peak value are more stable than the small peak to peak value. So when we move from $0.5°$ to $2°$ (first Web_MHD then Web_original and finally Web_PHD) the matching condition gets more stable and the close coupling has less impact on the performance of each tag.

Even though the Web_PHD has better performance in the close coupling, the Web_original has less variation in peak performance values of the tags in stack measurement. The reason is that the Web_original has wider track and smaller inner loop area in comparison with both Web_PHD and Web_MHD. The result of the stacked measurement shows that the Web_MHD has more variation in the peak values and also the bigger inner loop area between the designs.

As a consequence, the measurement results show that the Web_PHD is the optimum design for a good close coupling performance, since the read range and bandwidth has been improved compare to the original Web. Of course by changing some design parameters, the other features of the tag also will change, but now when the right matching point design has been achieved, the frequency shift can be fixed by changing the other parts of the tag (e.g. radiator part).

Certainly, the matching point design is not the only affecting factor to improve the close coupling performance, since all the design's parameters play important role in the performance of the tag. However, with respect to the time schedule of this thesis work, only the effect of matching point for improvement of close coupling effect has been studied, since this found to be primary aspect with respect to the theoretical modelling of the problem.

Chapter 6

6. Conclusions

This thesis involved the study about the effect of close coupling on the performance of the UHF RFID tags, when the tags are in close proximity to each other in stack (for instance, in a cloth shop jeans are labelled with RFID tags and are placed on top of each other). In addition, one practical design approach for improvement the performance of the tags in stack was introduced and the dominant factors which have influence on close coupling have been discussed.

The theoretical modelling and simulation of the tags in stack showed that when the tags are brought close to each other, the effect of mutual impedance will change the impedance of the antenna of the tags. Therefore, the impedance of the tag antennas is not anymore conjugate matched with the IC's impedance. Deviation from optimum matching condition will decrease the power delivered to the tag IC and the reader. Power drop was the main reason of decreasing the performance of the tags in stack. In most of the cases, the performance analysis of the tags in stack has been considered from theoretical point of view. In this thesis, the close coupling issue was explained from tag design perspective. The idea for performance enhancement of the tags in stack was to design an antenna that is less affected by adjacent tags to give more stable matching condition in stack environment.

From design perspective, there are many different parameters in design of a UHF tag antenna that affect the performance of the tag in close coupling situation. The elements such as skeleton of the antenna, size and shape, can have influence on performance of tag in stack, since all of them are involved in the antenna's impedance behaviour. We cannot consider the effect of each parameter individually on close coupling performance of antenna. For instance, it is not true to say that having a wider/narrower track or metal surface individually can decrease/increase the impact of close coupling. However, it is possible to achieve a good close coupling performance by improvement of the different

design factors. In this thesis, only the improvement of matching point for minimizing the close coupling effect has been studied since it was found to be primary aspect and has direct effect on matching condition. Moreover, changing all the design elements at the same time is not directly comparable.

The matching condition properties were discussed by using the S_{11} phase graph. It has been explained that the best matching can be achieved if the center point of the phase peak to peak value is on zero-cross line. However, the detuning effect of the material will change this condition and causes some offset from optimum phase graph. The acceptable shift from zero phase line, that still can keep the matching in good condition, depends on the fact that how big or small the peak to peak value is.

The design process of one Smartrac's product (Web), which has been designed for close coupling situations, was explained. To improve the performance of the Web tag in close coupling environment even further, the design of matching point of the antenna has been changed. Two alternative designs based on the original Web antenna have been created. By measuring the new version of the designs and comparing their results with the reference Web antenna, one optimal model (Web_PHD) was obtained that performed better than the reference Web in stack. The optimal model has higher peak to peak value for phase in S_{11} graph which can be interpreted as more stable matching condition compared to the reference Web antenna. Because, the higher peak to peak value of the phase graph allows more offset to the center point variation from zero phase line. So when a tag gets close to the other tag, the detuning effect of the other tag on the matching condition cannot push the phase graph that far from the optimal matching conditions. Whereas, the small peak to peak value for the phase, means that small shift on center point from zero line, can push the phase graph to non-optimal matching condition. In other word, in this case, the phase graph will easier get far from the optimal matching conditions by force of the external factors (such as material effect and closeness of the tags).

However, there are some limitation factors to have high peak to peak value. It is mentioned in the thesis that the peak to peak value of phase can be increased by decreasing the gap and width of the matching point in the design. Since always there are some production limits for making the antenna, the gap and width cannot be less than given manufacturing limits and so the peak to peak value cannot become as high as suggested by calculations. However, using high resolution antenna production methods make it possible to have narrower track.

Bibliography

[1] B. S. Guru and H. R. Hiziroglu, *Electromagnetic Field Theory Fundamentals*, 2nd ed., Cambridge University Press, 2004.

[2] D. M. Pozar, *Microwave Engineering*, 3rd ed., John Wiley & Sons Inc., 2005.

[3] D. K. Cheng, *Field and Wave Electromagnetics*, 2nd ed., Pearson, 2002.

[4] J. D. Kraus, and R. J. Marhefka, *Antennas, For All Applications*, 3r ed., McGRAW-HILL, 2002.

[5] C. A. Balanis, *Antenna Theory, Analysis and design*, 3rd ed., John Wiley & Sons Inc., United States of America, 2005.

[6] W. L. Stutzman, and G. A. Thiele, *Antenna Theory and Design*, 2nd ed. John Wiley & Sons Inc., United States of America, 1998.

[7] R. Ludwig, and G. Bogdanov, *RF Circuit Design, Theory and Application*, 2nd ed., Prentice Hall, United State of America, 2008.

[8] Electric field polarization forms, available at: http://upload.wikimedia.org/wikipedia/commons/2/2e/Linear_polarization_schematic.png?uselang=fi.

[9] D. M. Dobkin, *The RF in RFID, Passive UHF RFID in Practice*, Elsevier Inc., United States of America, 2008.

[10] H. Stockman, "Communication by Means of Reflected Power" *Proceedings of the IRE*, VOL. 36, NO. 10, October 1948.

[11] C. Z. Ning, *Antennas for Portable Devices*, John Wiley & Sons Inc., 2007.

[12] M. Bolic, D. Simplot-Ryl and I. Stojmenovic, *RFID Systems, Research Trends and Challenges*, John Wiley & Sons Inc., 2010.

[13] K. Penttila, *Studies towards Improving RFID Reader Performance*, PhD dissertation, Tampere University of Technology, 2006, ISBN 952-15-1617-8.

[14] K. Finkenzeller, *RFID Handbook*, 2nd ed., John Wiley & Sons Inc., 2004.

[15] EPC Radio-Frequency Identity Protocols, Class-1 Generation-2 UHF RFID, Version 1.1.0 (2005). http://www.gs1.org/gsmp/kc/epcglobal/uhfc1g2/uhfc1g2_1_1_0-standard-20071017.pdf.

[16] T. Koskelainen, *UHF Antenna Design and Design Validation Measurements*, Master of Science Thesis, Tampere University of Technology, 2007.

[17] K. V. Seshagiri Rao, P. V. Nikitin, and S. F. Lam, "Antenna design for UHF RFID tags: A review and a practical application", *IEEE Transactions of Antennas and Propagation*, Vol. 53, No. 12, December 2005.

[18] G. Marrocco, "The art of UHF RFID antenna design: Impedance-matching and size-reduction techniques", *IEEE Antennas and Propagation Magazine*, Vol. 50, No. 1, February 2008.

[19] Z. Tang, Y. He, Z. Huo, and B. Li, "The effects of Antenna Properties on read Distance in Passive backscatter RFID Systems", in *Proc. International Conference on Networks Security, Wireless communication and Trusted Computing*, 2009.

[20] S. Merilampi, *The Exploitation of Polymer Thick Films in Printing Passive UHF RFID Dipole Tag Antenna on Challenging Substrates*, PhD dissertation, Tampere University of Technology, 2011, ISBN 978-952-15-2584-1.

[21] T. Bauernfeind, K. Preis, G. Koczka, S. Maier, O. Biro, "Influence of the Non-Linear UHF RFID IC Impedance on the Backscatter Abilities of T-Match Tag Antenna Design", *IEEE Transactions on magnetic*, Vol. 48, No. 2, February 2012.

[22] J. H. Bae, K. T. Kim, W. Choi, and C. W. Park, *Current Trends and Challenges in RFID*, InTech Europe, 2011, ISBN: 978-953-307-356-9.

[23] Monza 5 tag chip Data sheet, www.Impinj.com, Accessed 23 January 2013.

[24] P. V. Nikitin, K. V. S. Rao, S. F. Lam, V. Pillai, R. Martinez, and H. Heinrich, "Power Reflection Coefficient Analysis for Complex Impedance in RFID Tag Design," *IEEE Trans. Microw. Theory Tech.*, vol. 53, No. 9, Sep. 2005.

[25] F. Lu, X. Chen and T. T. Ye, "Performance Analysis of Stacked RID Tags", *IEEE International conference on RFID*, 2009.

[26] T.W. Koo, D. Kim, J.I. Ryu, H. M. Seo, J. G. Yook, and J.C. Kim, "Design of a Label-Typed UHF RFID Tag Antennafor Metallic Objects", *IEEE Antennas and wireless propagation letters*, VOL. 10, 2011.

[27] Y. S. Chen, S. Y. Chen, and H. J. Li, "Analysis of Antenna Coupling in Near-Field Communication Systems", *IEEE Transactions on antennas and propagation*, VOL. 58, NO. 10, October 2010.

[28] L. Pierantoni, S. Lindenmeier, C. Ciandrini and T. Rozzi, "Efficient Modelling of the Near Field Coupling Between Phased Array Antennas", in *Proc.33rd European Microwave Conference, Munich 2003.*

[29] A. Buffi, P. Nepa, G. Manara, "Analysis of Near-Field Coupling in UHF-RFID Systems", *IEEE-APS topical conference on antennas and propagation in wireless communications (APWC)*, September 2011.

[30] X. Chen, F. Lu, and T. T. Ye, "The Weak Spots in Stacked UHF RFID Tags in NFC Applications", *IEEE International conference on RFID*, April 2010.

[31] S. M. Weigand, and D. M. Dobkin, “Multiple RFID Tag Plane Array Effects,” *IEEE Antennas and Propagation Society Symp.*, July 2006.

[32] D. B. Dobkin, and S. M. Weigrand, “UHF RFID and Tag Antenna Scattering, Part I: Experimental Results,” *Microwave Journal*, vol. 47, no. 5, May 2006.

[33] Y. Tanaka, Y. Umeda, O. Takyu, M. Nakayama, and K. Kodama, “Dependence of Antenna Impedance on Distance between UHF RFID Tags (In Japanese),” *IEICE Technical Report, AP2008-8*, Apr. 2004.

[34] H. C. Baker, and A. H. LaGrone, “Digital Computation of the Mutual Impedance Between Thin Dipoles,” *IRE Trans. Antennas Propag.*, vol. 10, No. 1109, Mar. 1962.

[35] Y. Tanaka, Y. Umeda, O.Takyu, M. Nakayama, and K. Kodama, ”Change of Read Range for UHF Passive RFID Tags in Close Proximity”, *IEEE International Conference on RFID*, 2009.

[36] H. Yojima, Y. Tanaka, Y. Umeda, O. Takyu, M. Nakayama, and K. Kodama, “Analysis of Read Range for UHF Passive RFID Tags in Close Proximity with Dynamic Impedance Measurement of Tag ICs”, *IEEE Radio and wireless symposium (RWS)*, January 2011.

[37] C. Reinhold, P. Scholz, W. John, and U. Hilleringmann, “Efficient Antenna Design of Inductive Coupled RFID-Systems with High Power Demand”, *Journal of communications,* VOL. 2, NO. 6, November 2007.

[38] K. C. Lee, and T. H. Chu, “Mutual Coupling Mechanisms within Arrays of Nonlinear Antennas”, *IEEE Transactions on electromagnetic compatibility*, VOL. 47, NO. 4, November 2005.

[39] D. M. Hall, *Antennas, Waves, and Circuits in Radio Frequency Identification*, PhD dissertation, The University of Adelaide, September 2011.

[40] H. J. Visser, *Array and Phased Array Antenna Basics* , John Wiley & Sons Inc., 2006.

[41] Tagformance Lite Measurement System, User guide, Rev 3.8.x (2011). http://voyantic.com/Tagformance%20Manual.pdf . Accessed 20 February 2013

[42] Application note, NXP Semiconductors, AN 1629 UHF RFID Label, Antenna Design, UHF Antenna Design, Rev. 1.0 — 05.09.2008.

[43] RFID Research Center, University of Arkansas, http://rfid.uark.edu/2058.asp Accessed 20 January 2013.

[44] Justin Patton, University of Arkansas, RFID research center, *ARC testing methodology, Version 1.37, December 7 2010*, "Document is available to anyone on request from the University of Arkansas" jpatton@walton.uark.edu.

[45] J. L. Volakis, C. C. Chen, and K. Fujimoto, *Small Antennas, Miniaturization Techniques and Applications*, McGrawHill, 2010, ISBN 978-0-07-162553-1.